AMERICAN SOCIETY FOR MICROBIOLOGY | mSystems®

RESEARCH ARTICLE

Systematic Analysis of Mobile Genetic Elements Mediating β-Lactamase Gene Amplification in Noncarbapenemase-Producing Carbapenem-Resistant *Enterobacterales* Bloodstream Infections

W. C. Shropshire,[a] A. Konovalova,[b] P. McDaneld,[c] M. Gohel,[a] B. Strope,[a] P. Sahasrabhojane,[a] C. N. Tran,[a] D. Greenberg,[d,e] J. Kim,[f] X. Zhan,[f] S. Aitken,[g] M. Bhatti,[h] T. C. Savidge,[i,j] T. J. Treangen,[k] B. M. Hanson,[l] C. A. Arias,[m] S. A. Shelburne[a,n]

[a]Department of Infectious Diseases and Infection Control, The University of Texas MD Anderson Cancer Center, Houston, Texas, USA
[b]Department of Microbiology and Molecular Genetics, McGovern Medical School, The University of Texas Health Science Center at Houston, Houston, Texas, USA
[c]Division of Pharmacy, The University of Texas MD Anderson Cancer Center, Houston, Texas, USA
[d]Department of Internal Medicine, UT Southwestern Medical Center, Dallas, Texas, USA
[e]Department of Microbiology, UT Southwestern Medical Center, Dallas, Texas, USA
[f]Department of Bioinformatics, UT Southwestern Medical Center, Dallas, Texas, USA
[g]Division of Pharmacy, Michigan Medicine at University of Michigan, Ann Arbor, Michigan, USA
[h]Department of Laboratory Medicine, The University of Texas MD Anderson Cancer Center, Houston, Texas, USA
[i]Department of Pathology and Immunology, Baylor College of Medicine, Houston, Texas, USA
[j]Department of Pathology, Texas Children's Hospital, Houston, Texas, USA
[k]Department of Computer Science, Rice University, Houston, Texas, USA
[l]Center for Infectious Diseases, School of Public Health, University of Texas Health Science Center, Houston, Texas, USA
[m]Department of Medicine, Houston Methodist Hospital, Houston, Texas, USA
[n]Department of Genomic Medicine, The University of Texas MD Anderson Cancer Center, Houston, Texas, USA

ABSTRACT Noncarbapenemase-producing carbapenem-resistant *Enterobacterales* (non-CP-CRE) are increasingly recognized as important contributors to prevalent carbapenem-resistant *Enterobacterales* (CRE) infections. However, there is limited understanding of mechanisms underlying non-CP-CRE causing invasive disease. Long- and short-read whole-genome sequencing was used to elucidate carbapenem nonsusceptibility determinants in *Enterobacterales* bloodstream isolates at MD Anderson Cancer Center in Houston, Texas. We investigated carbapenem nonsusceptible *Enterobacterales* (CNSE) mechanisms (i.e., isolates with carbapenem intermediate resistance phenotypes or greater) through a combination of phylogenetic analysis, antimicrobial resistance gene detection/copy number quantification, porin assessment, and mobile genetic element (MGE) characterization. Most CNSE isolates sequenced were non-CP-CRE (41/79; 51.9%), whereas 25.3% (20/79) were *Enterobacterales* with intermediate susceptibility to carbapenems (CIE), and 22.8% (18/79) were carbapenemase-producing *Enterobacterales* (CPE). Statistically significant copy number variants (CNVs) of extended-spectrum β-lactamase (ESBL) genes (Wilcoxon Test; *P*-value < 0.001) were present in both non-CP-CR *E. coli* (median CNV = 2.6×; $n = 17$) and *K. pneumoniae* (median CNV = 3.2×, $n = 17$). All non-CP-CR *E. coli* and *K. pneumoniae* had predicted reduced expression of at least one outer membrane porin gene (i.e., *ompC/ompF* or *ompK36/ompK35*). Completely resolved CNSE genomes revealed that IS*26* and IS*Ecp1* structures harboring $bla_{CTX\text{-}M}$ variants along with other antimicrobial resistance elements were associated with gene amplification, occurring in mostly IncFIB/IncFII plasmid contexts. MGE-mediated β-lactamase gene amplifications resulted in either tandem arrays, primarily mediated by IS*26* translocatable units, or segmental duplication, typically due to IS*Ecp1* transposition units. Non-CP-CRE strains were the most common cause of CRE bacteremia with carbapenem nonsusceptibility driven by concurrent porin loss and MGE-mediated amplification of $bla_{CTX\text{-}M}$ genes.

Editor Zackery Bulman, University of Illinois at Chicago

Address correspondence to S. A. Shelburne, sshelburne@mdanderson.org.

The authors declare a conflict of interest. CAA reports grants from NIH, Merck, MeMed Diagnostics and Entasis Therapeutics. In addition, CAA receives royalties from UpToDate and editor's stipend from American Society for Microbiology.

Received 31 May 2022
Accepted 26 July 2022
Published 29 August 2022

IMPORTANCE Carbapenem-resistant *Enterobacterales* (CRE) are considered urgent antimicrobial resistance (AMR) threats. The vast majority of CRE research has focused on carbapenemase-producing *Enterobacterales* (CPE) even though noncarbapenemase-producing CRE (non-CP-CRE) comprise 50% or more of isolates in some surveillance studies. Thus, carbapenem resistance mechanisms in non-CP-CRE remain poorly characterized. To address this problem, we applied a combination of short- and long-read sequencing technologies to a cohort of CRE bacteremia isolates and used these data to unravel complex mobile genetic element structures mediating β-lactamase gene amplification. By generating complete genomes of 65 carbapenem nonsusceptible *Enterobacterales* (CNSE) covering a genetically diverse array of isolates, our findings both generate novel insights into how non-CP-CRE overcome carbapenem treatments and provide researchers scaffolds for characterization of their own non-CP-CRE isolates. Improved recognition of mechanisms driving development of non-CP-CRE could assist with design and implementation of future strategies to mitigate the impact of these increasingly recognized AMR pathogens.

KEYWORDS carbapenem resistance, extended spectrum beta lactamase, mobile genetic elements, multi-drug resistance, osmoporin gene regulation, oxford nanopore technologies

Carbapenem-resistant *Enterobacterales* (CRE) infections are major public health challenges, particularly within vulnerable patient populations (1–6). There is a strong association between carbapenem resistance and resistance to other antibiotics (multidrug resistance; MDR), in part because carbapenem-resistant infections commonly occur in patients who have previously received multiple courses of antimicrobials (7, 8). A primary factor responsible for the dissemination of MDR phenotypes are mobile genetic elements (MGEs). These complex genetic structures (e.g., plasmids, transposons, and integrons) can mobilize carbapenem resistance determinants in addition to other antimicrobial resistance (AMR) genes that confer resistance to other classes of antibiotics such as fluoroquinolones, aminoglycosides, and other novel β-lactam/β-lactamase inhibitor combinations (9–13). In recent years, the development of long-read sequencing technologies has improved our understanding of the complexity, diversity, and prevalence of these MGEs as key drivers of MDR infections (13–20).

There are two general mechanisms by which MGEs contribute to the development of carbapenem resistance in *Enterobacterales* (21). MGEs can disseminate and mobilize carbapenemase genes, which encode enzymes that are able to hydrolyze the carbapenem β-lactam ring with sufficient efficiency to inactivate the drug, through horizontal gene transfer pathways (11, 22). For example, there are well documented associations of the *Klebsiella pneumoniae* carbapenemase (KPC) encoding gene being disseminated through isoforms of the Tn*3*-based Tn*4401* transposon (23). Interestingly, in recent years, surveillance studies have found that up to 50% of CRE detected lack a carbapenemase gene, i.e., are noncarbapenemase-producing CRE (non-CP-CRE) (1–3). Similar to MGEs key role in dissemination of carbapenemases, MGEs are also necessary for the dissemination of extended-spectrum β-lactamase (ESBL) and AmpC-like encoding enzymes that are both critical for the development of the non-CP-CRE phenotype (11, 12, 24–28).

Much of the existing knowledge regarding non-CP-CRE mechanisms is derived from laboratory passaging or serial, single isolate studies (24–28). These studies have shown that non-CP-CRE development typically involves increased expression or gene copy number of ESBL or AmpC-like enzymes in conjunction with outer membrane porin (*omp*) gene inactivation, which results in a reduced carbapenem concentration in the periplasmic space (24–28). Given that both ESBL and AmpC-like encoding genes are typically located in MGEs (11, 13, 29), an increase in β-lactamase gene copy number would seem to be feasible for a broad array of ESBL and AmpC-like positive *Enterobacterales*.

Recent data indicate that both non-CP-CRE and carbapenemase-producing *Enterobacterales* (CPE) undergo multiple genomic and transcriptomic adaptations prior to

becoming fully resistant to carbapenems (30, 31). A CRE US-based surveillance study published in 2020 found a large proportion of "unconfirmed" CRE infections (1) with clinical outcomes comparable to confirmed CRE infections, suggesting that many CRE isolates may have unstable, borderline carbapenem resistance (i.e., carbapenem intermediate resistance). Considering that this instability of carbapenem resistance phenotype may be due to heteroresistance arising from gene amplifications (32), it is critical to better understand the full breadth of carbapenem resistance genotypes. Therefore, one aim of this study is to characterize the union of *Enterobacterales* bloodstream isolates that are carbapenem-intermediate or carbapenem-resistant, hereinto referred to as carbapenem nonsusceptible *Enterobacterales* (CNSE), that contribute to carbapenem resistance in the hospital setting.

While many studies have shown associations of β-lactamase gene copy numbers with increased β-lactam phenotype (13–17, 33), to our knowledge, a systematic analysis of MGE-mediated β-lactamase-encoding gene amplifications in a large cohort of CNSE isolates using completed genome assemblies has not been performed. Given the repetitive, complex nature of MGEs that harbor these β-lactamase encoding genes, PCR detection or short-read sequencing approaches have had limited capacity to reveal the breadth of MGEs contributing to these varied CRE phenotypes.

Herein, we sought to systematically determine carbapenem resistance mechanisms by applying a combination of short- and long-read sequencing to a well-defined cohort of CNSE isolates. We found that non-CP-CRE isolates caused the vast majority of our CRE bacteremia cases and harbored MGEs with complex arrangements primarily of ESBLs, such as $bla_{\text{CTX-M}}$ variants, mediated by either IS*26* or IS*Ecp1* elements. There was a statistically significant association of ESBL amplification in conjunction with *omp* gene disruption in non-CP-CR *Escherichia coli* and *Klebsiella pneumoniae*. Using Oxford Nanopore Technologies (ONT) long-read sequencing, we clarified that ESBL amplification was associated with IS*26*-mediated "translocatable units" (TUs) and IS*Ecp1* "transposition units" (TPUs) in both non-CP-CR *Escherichia coli* and *Klebsiella pneumoniae*, thereby improving the understanding of mechanisms underlying the non-CP-CRE phenotype.

RESULTS

Molecular epidemiology of carbapenem-nonsusceptible *Enterobacterales* (CNSE) causing bacteremia at MD Anderson Cancer Center (MDACC). There were 1,632 unique *Enterobacterales* bloodstream infections (BSIs) at our institution from July 2016 to June 2020. The leading causes were *Escherichia coli* (939/1,632; 57.5%) followed by *Klebsiella pneumoniae* (338/1,632; 20.7%) and *Enterobacter* spp. (159/1,632; 9.7%). A total of 5.2% (85/1,632) were CDC-defined carbapenem-resistant with an additional 1.8% (29/1,632) having intermediate carbapenem resistance based on CLSI breakpoints (i.e., carbapenem-intermediate *Enterobacterales* [CIE]), resulting in a total 7.0% (114/1,632) that were carbapenem-nonsusceptible *Enterobacterales* (CNSE) as initially determined by the MDACC clinical microbiology laboratory. When stratifying the causal species of BSI by carbapenem nonsusceptibility, 39.5% (45/114) of CNSE were *Escherichia coli* followed by *Klebsiella pneumoniae sensu stricto* (30.7%; 35/114) and *Enterobacter* spp. (16.7%; 19/114). We found a statistically significant difference in carbapenem nonsusceptibility by species (Fisher's exact test, P value < 0.001) with a higher prevalence of *K. pneumoniae* BSIs (10.4%; 35/338) that were carbapenem-nonsusceptible compared to *E. coli* (4.8%; 45/939), consistent with other CRE surveillance studies in the United States (1, 2, 34).

A total of 91% (104/114) CNSE BSI isolates were present in our sample collection (Fig. 1). Of these 104 CNSE BSI isolates, we confirmed at least ertapenem MIC intermediate interpretations for 37/42 *E. coli* (88%), 28/32 *K. pneumoniae* (88%), 8/15 *Enterobacter* spp. (53%), and 6/15 other *Enterobacterales* (40%), with the remaining isolates being considered unconfirmed-CNSE (Fig. 1). Thus, we had 79 CNSE-confirmed BSI isolates which underwent whole-genome sequencing (WGS) to determine respective carbapenem nonsusceptibility genotypes. Only 23% of BSI isolates (18/79) had a confirmed carbapenemase, whereas the majority were non-CP-CRE (41/79; 52%) or CIE (20/79; 25%) based on WGS analysis and carbapenem MIC determination (Fig. 1). We identified 17 CNS*Ec* bacteremia cases that had a

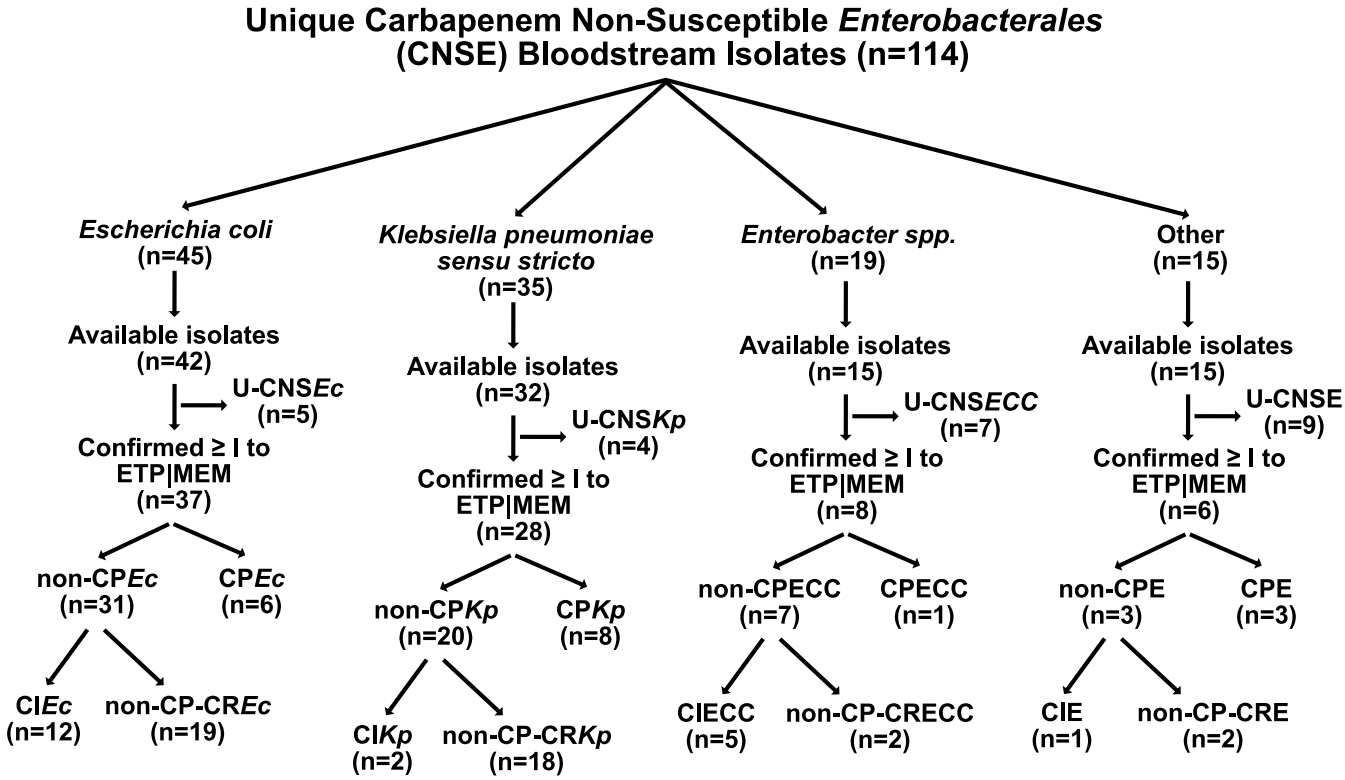

FIG 1 Selection and delineation of carbapenem-nonsusceptible *Enterobacterales* bloodstream infection isolates. Total isolates per group included in parenthesis. U-CNS, unconfirmed carbapenem-nonsusceptible; non-CP, noncarbapenemase-producing; non-CP-CR, noncarbapenemase-producing carbapenem-resistant; CP, carbapenemase producing; *Ec*, *Escherichia coli*; *Kp*, *Klebsiella pneumoniae*; ECC, *Enterobacter cloacae* complex; E, *Enterobacterales*.

prior initial carbapenem-susceptible *E. coli* bacteremia infection which had tested positive for ESBL production in 16/17 cases. Interestingly, all 17 of these CNS*Ec* isolates were carbapenemase-negative. Similarly, 5/6 CNS*Kp* that were preceded by an initial carbapenem-susceptible *K. pneumoniae* bacteremia were carbapenemase-negative as well. When focusing on clinical features, there were no statistically significant differences in age, gender, country of origin, recent travel history, or predicted source of BSI across each of the CNSE categories, albeit there were a small number of observations per category (Table S1).

Enterobacter spp. were the third most prevalent group of CNSE BSI isolates with all isolates belonging to the *Enterobacter cloacae* complex (ECC) (Table S2). The majority of CNSE-confirmed ECC had CIE phenotypes (5/8; 63%), with only one carbapenemase-producing ECC (CPECC) isolate harboring bla_{KPC-2} (MB8139), and two noncarbapenemase-producing carbapenem-resistant ECC (non-CP-CRECC). With regard to the non-CP-CRECC isolates, both had outer membrane porin (*omp*) gene disruptions with one non-CP-CRECC (MB5921) containing an ESBL gene (bla_{SHV-12}). The other non-CP-CRECC isolate (MB6956) had a carbapenem-resistant mechanism that likely involved an overexpressed chromosomal *ampC* gene (bla_{CMH}) due to an *ampD*/*ampE* fusion mutation, with the inactivation of the AmpD gene predicted to result in AmpC derepression (35) (Table S2). The six other *Enterobacterales* spp. detected in our cohort included 3 CPE (*Klebsiella* spp. not including *K. pneumoniae sensu stricto*), 2 non-CP-CRE (1 *K. aerogenes* and 1 *Citrobacter freundii*), and 1 CIE (*Serratia marcescens*) (Table S2). We focused the remainder of this study on the two most common, clinically relevant species in our cohort, *E. coli* and *K. pneumoniae*, and the putative mechanisms responsible for their carbapenem-nonsusceptible phenotypes.

Characterization of carbapenem resistance mechanisms among CNS *E. coli* and *K. pneumoniae* isolates. There were 37 unique carbapenem-nonsusceptible *E. coli* (CNS*Ec*) bacteremia isolates with 6 CP*Ec* (16%), 19 non-CP-CR*Ec* (51%), and 12 CI*Ec* (32%) (Table S2). A summary of molecular features of CNS*Ec* is provided in Table S3. Core gene alignment inferred, maximum-likelihood phylogenetic trees for CNS*Ec* isolates with carbapenem

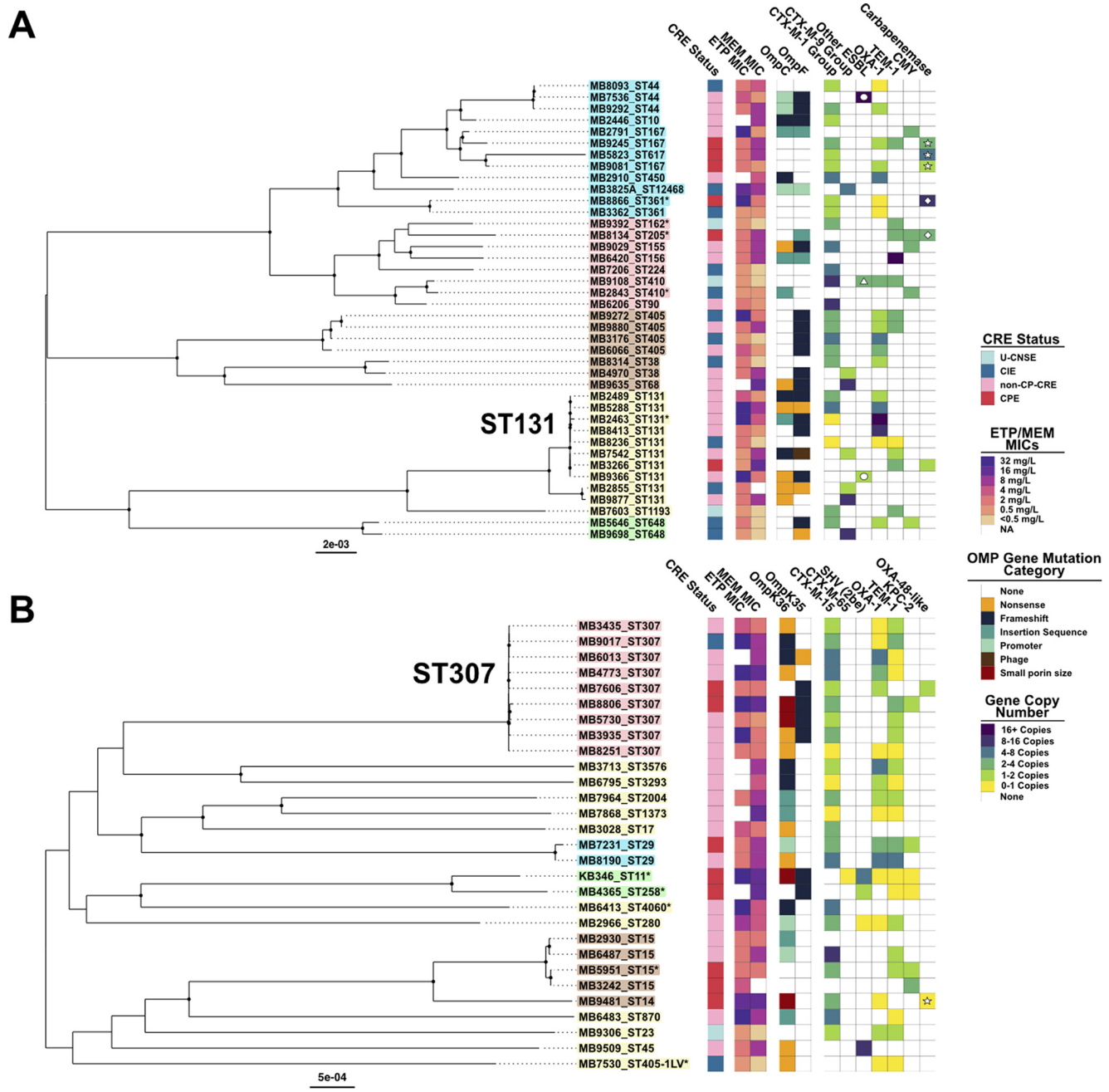

FIG 2 Population structure of *E. coli* and *K. pneumoniae* bacteremia isolates with phenotype/genotype data. Core gene alignment inferred; midpoint rooted maximum likelihood phylogenies. Circles at internal nodes indicate UFBoot values with ≥95% support. Tip label background color corresponds to nested population structure identified using hierarchical clustering of sequence data with rhierbaps. Carbapenem resistance status, ertapenem (ETP) and meropenem (MEM) MICs (μg/mL), outer membrane porin gene mutation status, and gene copy number estimate are presented in columnar data from left to right and labeled in the legend, respectively. An asterisk (*) adjacent to the tip label indicates isolates with only draft assembly. Samples with ETP or MEM MIC results labeled "NA" indicate isolates that did not have these data recorded by the MDACC clinical microbiology lab. (A) *E. coli* population structure (n = 40). Circles in the "Other ESBL" column indicate bla_{TEM} variants whereas the triangle indicates bla_{SHV-12}. Stars in the "Carbapenemase" column indicate bla_{NDM-5}, diamonds indicate $bla_{OXA-48-like}$, and absence of shape indicates bla_{KPC-2}. Tip labels correspond to hierarchical population structure cluster by phylogroup with A (n = 12; blue), B2 (n = 11; yellow), D (n = 7; brown), B1/C (n = 8; pink), and F (n = 2; green) (B) *K. pneumoniae* population structure (n = 29). The isolate with a star in the "OXA-48-like" ($bla_{OXA-48-like}$) column indicates cocarriage of bla_{NDM-1} with 1 to 2 copies.

susceptibility profile, outer membrane porin gene (*omp*) mutation status, and β-lactamase gene presence/absence with copy number estimates are shown in Fig. 2A. Hierarchical clustering of core gene SNPs resulted in five clusters, indicated by tip label color (Fig. 2A), that segregate isolates based on phylogroups A (n = 12), B2 (n = 11), D (n = 7), B1/C (n = 8), and F (n = 2) (36). The most identified sequence type (ST) among CNS*Ec* was the uropathogenic

strain ST131 (10/37; 27%). The mean pairwise core gene SNP difference was 57,355 SNPs (standard deviation [SD] = 25,621 SNPs). There were only two clinical isolates, MB9272 and MB9880, that had less than 50 core gene SNP differences (18 SNPs), further indicating minimal clonal infections among the *E. coli* strains in our cohort.

Among the six CP*Ec* isolates, three isolates from phylogroup A harbored $bla_{\text{NDM-5}}$, two unique ST isolates harbored plasmid borne $bla_{\text{OXA-48-like}}$ genes (MB8866 = $bla_{\text{OXA-232}}$ and MB8134 = $bla_{\text{OXA-181}}$), and one isolate (MB3266) carried a plasmid-borne Tn*4401a* transposon harboring $bla_{\text{KPC-2}}$. Only one CP*Ec* (MB8134) had an *omp* mutation (IS*2* insertion within *ompF*) (Fig. 2A). Regarding non-CP-CR*Ec*, 79% (15/19) of isolates were ESBL-positive. The most common β-lactamases detected in non-CP-CR*Ec* were CTX-M-1 group variants (7 $bla_{\text{CTX-M-15}}$ and 3 $bla_{\text{CTX-M-55}}$), CTX-M-9 group variants (3 $bla_{\text{CTX-M-27}}$, 1 $bla_{\text{CTX-M-14}}$, and 1 $bla_{\text{CTX-M-195}}$), $bla_{\text{OXA-1}}$ (n = 8), $bla_{\text{TEM-1}}$ (n = 4), and bla_{CMY} variants (n = 2). One ST131 non-CP-CR*Ec* isolate (MB9366) carried a novel bla_{TEM} variant (p.M182T, p.G238S, p.E240K, p.S243A, p.S270G), which was identified as an ESBL-E by the MDACC clinical microbiology lab and has an antibiogram that resembles an ESBL-E (Table S4). In contrast to the low prevalence of *ompC* and *ompF* mutations detected in CP*Ec*, all 19 non-CP-CR*Ec* isolates had at least one *ompC* or *ompF* mutation except for MB6206 (Fig. 2A; Table S3), which had an IS*Ecp1*-$bla_{\text{CTX-M-55}}$ insertion into the histidine kinase gene *envZ*, a known regulator of *ompC* and *ompF* expression (37). Consistent with EnvZ inactivation, immunoblot analysis confirmed a significant reduction of OmpC/OmpF in MB6206 (Fig. S1). Furthermore, 63% (12/19) of non-CP-CR*Ec* isolates were double mutant *ompC/ompF* isolates (Fig. 2A; Table S3). Similar to non-CP-CR*Ec*, 11/12 (91.7%) of CI*Ec* were ESBL carriers with eight CTX-M-1 group variants (7 $bla_{\text{CTX-M-15}}$; 1 $bla_{\text{CTX-M-1}}$) and three CTX-M-9 group variants (2 $bla_{\text{CTX-M-14}}$; 1 $bla_{\text{CTX-M-27}}$). Other common β-lactamases detected in CI*Ec* were $bla_{\text{OXA-1}}$ (n = 7) and bla_{CMY} (n = 2) variants. Relative to non-CP-CR*Ec* (18/19), CI*Ec* *ompC* and *ompF* mutations were less prevalent (7/12; 58%; Fisher's exact test P value = 0.02) with only two strains (16%) having mutations in both genes.

There were 28 unique carbapenem-nonsusceptible *K. pneumoniae* (CNS*Kp)* bacteremia isolates with eight CP*Kp* (29%), 18 non-CP-CR*Kp* (64%), and two CI*Kp* (7%) (Table S2). The core population structure of CNS*Kp* BSI isolates is presented in Fig. 2B The finding that 64% CR*Kp* were noncarbapenemase producers was noteworthy given that in most US-based CRE surveillance studies, the majority of CR*Kp* are carbapenemase-positive (1, 34). Indeed, for our cohort, the proportion of non-CP-CR*Kp* (18/28) was comparable to non-CP-CR*Ec* isolates (19/37; χ-squared test statistic = 0.62; P-value = 0.4). The most common sequence type identified was the ST307 lineage (9/28; 32%) followed by 18% (5/28) belonging to clonal group 15 (CG15). Hierarchical clustering demonstrated that, apart from ST307 and CG15 isolates, most CNS*Kp* belonged to single, long-branching isolates (Fig. 2B), indicating limited genetic relatedness. In support of this observation was a mean pairwise core gene SNP difference of 22,141 SNPs (SD = 7,864) with the minimum pairwise core gene SNP distance between our CNS*Kp* isolates being 38 SNPs between two ST15 isolates (MB5951 and MB3242). Among CP*Kp*, six isolates encoded $bla_{\text{KPC-2}}$, one isolate (MB7606) encoded $bla_{\text{OXA-181}}$, and one isolate (MB9481) encoded two carbapenemases, $bla_{\text{NDM-1}}$ and $bla_{\text{OXA-48}}$. The *ompK36* or *ompK35* mutations (i.e., *ompC* and *ompF K. pneumoniae* homologs, respectively) that would be predicted to affect outer membrane porin function were present in 5/8 (62.5%) CP*Kp*. Almost all non-CP-CR*Kp* carried $bla_{\text{CTX-M-15}}$ (16/18; 84%) with one such isolate having a novel, single amino acid $bla_{\text{CTX-M-15}}$ variant (MB6013; p.P269S). The β-lactamase-encoding genes $bla_{\text{OXA-1}}$ (n = 14) and $bla_{\text{TEM-1}}$ (n = 10) were also commonly detected in non-CP-CR*Kp*. All non-CP-CR*Kp* isolates had an *ompK36* mutation with 16.6% (3/18) also having an *ompK35* mutation (Fig. 2B). Only 2 CI*Kp* isolates were identified, both having *ompK36* disrupted ORFs with one isolate (MB9017) harboring $bla_{\text{CTX-M-15}}$, $bla_{\text{OXA-1}}$, and $bla_{\text{TEM-1,}}$ and the other isolate harboring only $bla_{\text{OXA-1}}$ and $bla_{\text{TEM-1.}}$ Taken together, the core population structure indicates disparate CNS *E. coli* and *K. pneumoniae* sequence types with little evidence of clonal outbreaks in addition to a high prevalence of ESBL-encoding genes with universal predicted *omp* gene disruption within non-CP-CRE isolates.

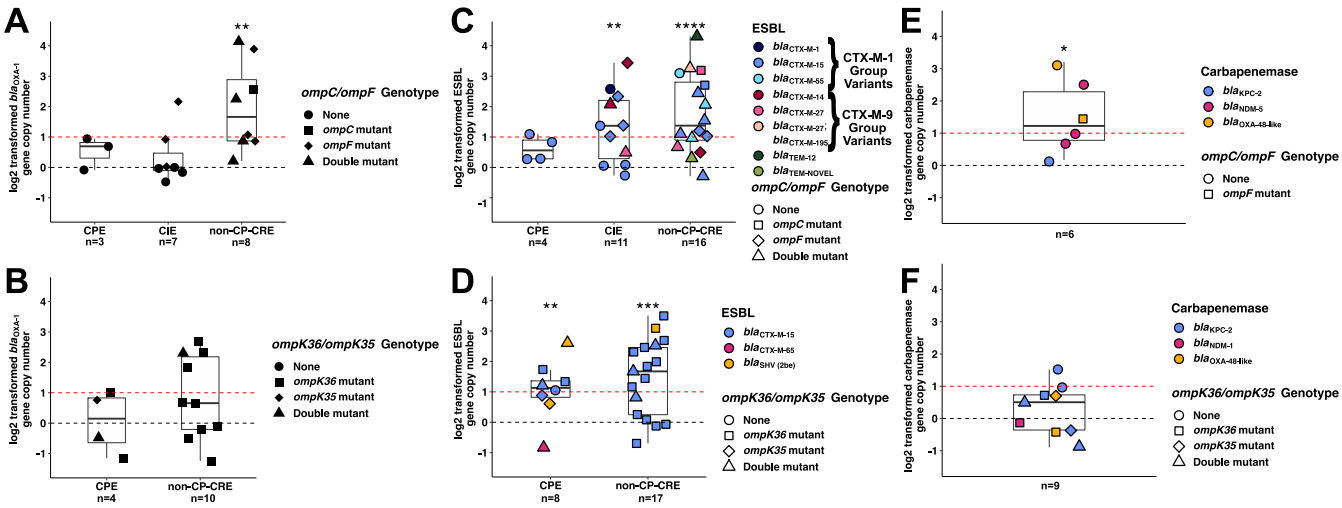

FIG 3 Log_2 transformed β-lactamase gene copy numbers with outer membrane porin gene mutation profile stratified by carbapenem-nonsusceptible (CNS) definitions. (A, C, and E) *Escherichia coli* and (B, D, and F) *Klebsiella pneumoniae* CNS isolates. Black dotted horizontal line at y = 0 is equivalent to 1× gene copy; Red dotted horizontal line at y = 1 is equivalent to 2× gene copy. Totals below categories reflect gene counts. CPE, carbapenemase-producing *Enterobacterales*; CIE, carbapenem-intermediate *Enterobacterales*; non-CP-CRE, noncarbapenemase-producing carbapenem-resistant *Enterobacterales*. One sample, one-sided, Wilcoxon test on nontransformed copy number estimates to determine statistically significant gene copy number amplifications (i.e., >1 copy) with *P*-values: *, $P < 0.05$; **, $P < 0.01$; ***, $P < 0.001$; ****, $P < 0.0001$.

Copy number variant profiling of β-lactamase-encoding genes in CNSE. An increase in copy number of ESBL, AmpC-like, and narrow-spectrum β-lactamase-encoding genes has been previously documented as contributing to CNSE development (13, 25, 27, 28). Thus, we next sought to comprehensively assess the presence of β-lactamase gene amplifications and their associations with each carbapenem nonsusceptibility profile (Table S5). To this end, we analyzed β-lactamase-encoding gene copy number variants (CNVs) and determined which CNSE groups had median CNV estimates greater than baseline (i.e., 1 copy) (Fig. 3). Non-CP-CR*Ec* contained statistically significant increases in gene copy numbers of the narrow spectrum β-lactamase-encoding gene bla_{OXA-1} (median CNV = 3.4×; one-sample, one-sided, Wilcoxon test *P*-value = 0.004) (Fig. 3A) that were not found in other CNS*Ec* categories nor in any of the CNS*Kp* groups (Fig. 3B). Both non-CP-CR*Ec* (median CNV = 2.6×; Wilcoxon test *P*-value <0.0001) and non-CP-CR*Kp* (median CNV = 3.2×; Wilcoxon test *P*-value <0.001) had statistically significant increases in ESBL gene copy numbers shown in Fig. 3C and D, respectively. Notably 80% (12/15) and 64% (11/17) of ESBL-positive, non-CP-CR*Ec* and non-CP-CR*Kp*, respectively, had an estimated ≥2 copies of ESBL-encoding genes (Table S5). Similar to non-CP-CR*Ec*, CI*Ec* also had a statistically significant increase in ESBL gene copy number (median CNV = 2.6×; *P*-value <0.001). Amplification of carbapenemase-encoding genes (median CNV = 2.4×; *P*-value = 0.02) was also detected in CP*Ec* (Fig. 3E), which was not evident in CP*Kp* (median CNV = 1.4×; *P*-value = 0.2) (Fig. 3F). While there was notably high bla_{TEM-1b} amplification in non-CP-CR*Ec* (median CNV = 11.5×), this did not reach statistical significance likely due to small number of observations (n = 4) and high variance in CNV estimates (Fig. S2A); whereas non-CP-CR*Kp* did not have evidence of bla_{TEM-1b} amplification (Fig. S2B). Lastly, bla_{CMY} amplification was present in CNS*Ec* with all five bla_{CMY}-positive isolates having estimated copy numbers greater than two (Table S5). Thus, a broad range of β-lactamases had evidence of gene copy number amplifications with statistically significant ESBL gene amplifications being detected in both non-CP-CR*Ec* and non-CP-CR*Kp* isolates.

Genomic structures contributing to carbapenem resistance development in CNSE cohort. Having quantified the extent of β-lactamase amplification across each of the CNSE groups, we used long-read ONT sequencing to complete genomes of 65 CNSE isolates (Table S2) in order to resolve the putative MGEs associated with mobilization and amplification of β-lactamase-encoding genes. We initially characterized the MGEs in CNSE isolates harboring β-lactamase genes greater than or equal to 2× copies (Fig. 3) with results shown for CNS*Ec* (Table 1) and CNS*Kp* (Table 2). When we subset these isolates with

TABLE 1 Summary of carbapenem nonsusceptibility mechanisms for *E. coli* with β-lactamase amplifications[a]

Carbapenem resistance status	Sample	MLST	*ompC*[b]	*ompF*[b]	*envZ/ompR*[b]	ESBL CNV	OXA-1 CNV	CMY CNV	TEM CNV	CARB CNV	MGE + β-lactamase[c]	Genomic context	Amp. pred.[d]
CI*Ec*	MB8314	38	ND	ND	ND	2.6	1.0	ND	ND	ND	IS*Ecp1*-$bla_{CTX-M-15}$/bla_{OXA-1}; IS*Ecp1*-$bla_{CTX-M-15}$	Chromosome	MGE
	MB7206	224	ND	ND	ND	6.0	ND	ND	ND	ND	IS*26*-$bla_{CTX-M-1}$	Chromosome	MGE
	MB3176	405	ND	p.Y254E fsX3	ND	5.0	4.5	ND	ND	ND	IS*26*-v1-$bla_{CTX-M-15}$/bla_{OXA-1}	Plasmid	MGE
	MB9272	405	ND	p.Y254E fsX3	ND	2.0	1.9	ND	2.0	ND	IS*26*-$bla_{CTX-M-15}$/bla_{OXA-1}/bla_{TEM-1b}	Plasmid	PCN
	MB2843	410	Insertion sequence	ND	ND	ND	ND	4.0	ND	ND	IS*Ecp1*-bla_{CMY-2}	Chromosome	MGE
	MB5646	648	ND	p.A238G fsX7	ND	2.6	1.0	1.9	ND	ND	IS*Ecp1*-$bla_{CTX-M-15}$; IS*26*-bla_{OXA-1}; bla_{CMY-4}	Plasmid	PCN
	MB9698	648	ND	p.L15X	ND	10.8	ND	ND	ND	ND	IS*Ecp1*-$bla_{CTX-M-14}$	Chromosome	MGE
	MB3825A	12468	IS*1A* 50 bp +1 ATG	IS*1A* 101 bp +1 ATG	ND	4.2	ND	ND	ND	ND	IS*Ecp1*-$bla_{CTX-M-14}$	Chromosome + plasmid	MGE
Non-CP-CR*Ec*	MB2446	10	p.F212R fsX30	p.Y26W fsX9	ND	2.0	ND	ND	ND	ND	IS*Ecp1*-$bla_{CTX-M-55}$	Plasmid	MGE + PCN*
	MB7536	44	IS*1F* 66 bp +1 ATG	p.Y62Y fsX1	ND	19.8	ND	ND	19.0	ND	IS*26*-bla_{TEM-12} (Tn3-like transposon)**	Plasmid	MGE + PCN
	MB9292	44	IS*1R* 49 bp +1 ATG	p.S46P fsX15	ND	2.9	1.2	ND	ND	ND	IS*26*-$bla_{CTX-M-15}$/bla_{OXA-1}	Plasmid	MGE
	MB9635	68	p.E237X	p.S164V fsX12	ND	9.6	ND	ND	ND	ND	IS*26*-$bla_{CTX-M-27}$; IS*26*-v1-$bla_{CTX-M-195}$**	Plasmid	PCN
	MB6206	90	ND	ND	c.191_192ins IS*Ecp1* TPU	8.6	ND	ND	ND	ND	IS*Ecp1*-$bla_{CTX-M-55}$	Chromosome + plasmid	MGE + PCN
	MB5288	131	p.Y250X	p.Q88X	ND	5.4	4.7	ND	ND	ND	IS*26*-$bla_{CTX-M-15}$/bla_{OXA-1}	Chromosome	MGE
	MB2463	131	c.496_497 insIS*26* TU	p.N183T fsX58	ND	0.8	17.7	ND	ND	ND	IS*26*-$bla_{CTX-M-15}$/bla_{OXA-1}	Chromosome	MGE
	MB8413	131	ND	p.N183T fsX58	ND	ND	14.9	ND	ND	ND	IS*26*-bla_{OXA-1}	Chromosome	MGE
	MB2489	131	p.Y170K fsX2	p.F102T fsX6	ND	2.2	1.8	ND	ND	ND	IS*26*-$bla_{CTX-M-15}$/bla_{OXA-1}	Chromosome + plasmid	MGE + PCN
	MB9877	131	p.Q82X	ND	ND	9.1	ND	ND	ND	ND	IS*26*-$bla_{CTX-M-27}$	Plasmid	MGE + PCN*
	MB9029	155	p.Q172X	p.A95A fsX75	ND	4.2	ND	2.6	ND	ND	IS*Ecp1*-$bla_{CTX-M-55}$; IS*Ecp1*-bla_{CMY-2}	Chromosome + plasmid	MGE + PCN
	MB6420	156	c.844_845 insIS*10L*	c.44_45 insIS*10L*	ND	ND	ND	ND	152.3	ND	Tn*2*-bla_{TEM-1b}	Chromosome	MGE
	MB2791	167	c.908_909 insIS*Ec35*	c.698_699 insIS*Ec35*	ND	ND	ND	2.9	ND	ND	IS*IR*-bla_{CMY-42}	Plasmid	PCN
	MB6066	405	ND	p.Y254E fsX3	ND	2.3	2.1	ND	ND	ND	IS*26*-$bla_{CTX-M-15}$/bla_{OXA-1}	Plasmid	PCN
	MB9880	405	ND	p.Y254E fsX3	ND	2.0	1.8	ND	4.0	ND	IS*26*-$bla_{CTX-M-15}$/bla_{OXA-1}; IS*26*-v1-bla_{TEM-1b}	Plasmid	MGE + PCN

(Continued on next page)

TABLE 1 (Continued)

Carbapenem resistance status	Sample	MLST	*ompC*[b]	*ompF*[b]	*envZ/ompR*[b]	ESBL CNV	OXA-1 CNV	CMY CNV	TEM CNV	CARB CNV	MGE + β-lactamase[c]	Genomic context	Amp. pred.[d]
	MB2910	450	p.L32L fsX3	ND	ND	6.5	5.9	ND	ND	ND	IS*26*-$bla_{CTX\text{-}M\text{-}15}$/$bla_{OXA\text{-}1}$	Plasmid	MGE + PCN
CP*Ec*	MB3266	131	ND	ND	ND	ND	ND	ND	2.6	1.1	Tn*4401a*-$bla_{KPC\text{-}2}$; IS*26*-$bla_{TEM\text{-}1b}$	Plasmid	MGE
	MB9245	167	ND	ND	ND	2.1	1.9	ND	2.2	2.0	IS*26*-$bla_{NDM\text{-}5}$; IS*26*-$bla_{CTX\text{-}M\text{-}15}$/$bla_{OXA\text{-}1}$; IS*26*-$bla_{TEM\text{-}1b}$	Plasmid	PCN
	MB8134[e]	205	ND	c.1049_1050 insIS2	ND	ND	ND	2.8	2.8	2.8	IS*3000*-$bla_{OXA\text{-}181}$; $bla_{CMY\text{-}42}$; $bla_{TEM\text{-}1b}$	NA	NA
	MB8866[e]	361	ND	ND	ND	1.2	0.9	ND	ND	9.2	IS*1* × *1*-$bla_{OXA\text{-}232}$; $bla_{CTX\text{-}M\text{-}15}$	NA	NA
	MB5823	617	ND	ND	ND	1.2	ND	ND	ND	5.9	IS*26*-$bla_{NDM\text{-}5}$; IS*Ecp1*-$bla_{CTX\text{-}M\text{-}15}$	Chromosome + plasmid	MGE + PCN

[a]ND, not detected; MGE, mobile genetic element; PCN, plasmid copy number; NA, not applicable.

[b]Outer membrane porin mutations for frameshifts and insertions/deletions notated in amino acid mutation nomenclature. Otherwise, insertion sequence (IS) disruptions noted in nucleotide space. IS notated with 'bp + 1 ATG' indicate IS insertions upstream of outer membrane porin (*omp*) gene in promoter region.

[c]β-lactamase genes without preceding insertion sequence and NOT in the same mobilization unit (delimited by "/") do not have sufficient genomic context for MGE estimate. **,Cannot differentiate copy number variants from homologs (i.e., genes with > 95% identity).

[d]Amp. pred. = amplification prediction. Plasmid copy number contributions were based on normalized coverage depths of full-length plasmid harboring β-lactamase = 1.5×, which indicates approximately 50% of the population has 2 copies of the β-lactamase-positive plasmid. *,MGE + PCN context resolved in part through extraction of individual long reads using SVants (74).

[e]Incomplete and/or short-read assemblies only preclude an estimate of genomic context of β-lactamase gene amplification.

TABLE 2 Summary of carbapenem nonsusceptibility mechanisms for *K. pneumoniae* with β-lactamase amplifications[a]

Carbapenem resistance status	Sample	MLST	*ompK36*[b]	*ompK35*[b]	ESBL CNV	OXA-1 CNV	TEM-1 CNV	CARB CNV	mGE + β-lactamase[c]	Genomic context	Amp. Pred.[d]
CI*Kp*	MB9017	307	p.D51R fsX37	ND	2.3	1.0	2.2	ND	IS*26*-$bla_{CTX-M-15}$/bla_{OXA-1}/bla_{TEM-1b}	Chromosome	MGE
Non-CP-CR*Kp*	MB6487	15	IS*Ecp1* 18 bp +1 ATG	ND	11.4	ND	1.1	ND	IS*Ecp1*-$bla_{CTX-M-15}$; Tn*2*-like transposon	Chromosome + plasmid	MGE
	MB3028	17	p.Q66X	ND	2.2	ND	ND	ND	IS*26*/IS*Ecp1*-$bla_{CTX-M-15}$	Plasmid	PCN
	MB8190	29	p.Q310X	ND	5.5	6.4	4.2	ND	IS*Ecp1*-$bla_{CTX-M-15}$/bla_{OXA-1}/bla_{TEM-1b}	Chromosome + plasmid	MGE
	MB9509	45	p.L305X	ND	8.5	ND	ND	ND	IS*903B*-bla_{SHV-7}**	Plasmid	PCN
	MB2966	280	IS*Ecp1* TPU 1 bp +1 ATG	ND	2.7	0.9	2.0	ND	IS*Ecp1*-$bla_{CTX-M-15}$/bla_{TEM-1b}; IS*26*-bla_{OXA-1}	Chromosome + plasmid	MGE
	MB6013	307	p.D33E fsX4	p.W230X	5.7	4.9	1.0	ND	IS*26*-$bla_{CTX-M-15}$/bla_{OXA-1}; IS*26*-bla_{OXA-1}	Plasmid	MGE
	MB4773	307	p.Q70X	ND	4.0	3.6	0.9	ND	IS*26*-$bla_{CTX-M-15}$/bla_{OXA-1}; IS*26*-bla_{TEM-1b}	Plasmid	MGE
	MB3935	307	p.E87X	p.G208VfsX6	3.2	ND	1.1	ND	IS*Ecp1*-$bla_{CTX-M-15}$; Tn*2*-like transposon	Plasmid	MGE
	MB6483	870	c.950_951 insIS*26* TU	ND	5.0	ND	0.9	ND	IS*26*-$bla_{CTX-M-15}$/bla_{TEM-1b} IS*Ecp1*-$bla_{CTX-M-15}$;	Chromosome + plasmid	MGE
	MB7964	2004	c.1115_1116 insIS*Ecp1* TPU	ND	3.6	1.7	1.6	ND	IS*Ecp1*-$bla_{CTX-M-15}$/bla_{OXA-1}/bla_{TEM-1b}	Chromosome + plasmid	MGE
	MB6413[e]	4060	p.A12A fsX11	ND	6.4	ND	ND	ND	IS*Ecp1*-$bla_{CTX-M-15}$	NA	NA
CP*Kp*	KB346[e]	11	p.G134_D135 dup	p.L28LfsX36	0.6 (CTX-M) 6.1 (SHV)	0.7	0.5	0.6	Tn*4401a*-bla_{KPC-2}; $bla_{CTX-M-65}$; bla_{SHV-12}; bla_{OXA-1}; bla_{TEM-1b};	NA	NA
	MB9481	14	p.G134_D135 dup	ND	3.3	0.5	ND	0.9 (NDM) 0.8 (OXA-48)	Tn*125*-bla_{NDM-1}; IS*Ecp1*-$bla_{CTX-M-15}$; IS*Kpn26*-bla_{OXA-48}; IS*26*-bla_{OXA-1}	Chromosome + plasmid	MGE
	MB3242	15	ND	ND	ND	ND	ND	2.9	Tn*4401a*-bla_{KPC-2}	Plasmid	PCN
	MB5951[e]	15	ND	ND	2.1	ND	1.8	2.0	Tn*4401a*-bla_{KPC-2}; IS*Ecp1*-$bla_{CTX-M-15}$; bla_{TEM-1b}	NA	NA
	MB7231	29	ISKpn14 46 bp +1 ATG	ND	2.4	2.0	2.7	1.7	Tn*4401a*-bla_{KPC-2}; IS*Ecp1*-$bla_{CTX-M-15}$/bla_{OXA-1}/bla_{TEM-1b}	Chromosome + plasmid	MGE + PCN
	MB8806	307	p.G134_D135 dup	p.G208VfsX6	2.3	ND	2.4	1.4	Tn*4401a*-bla_{KPC-2}; IS*Ecp1*-$bla_{CTX-M-15}$ IS*26*-bla_{TEM-1b}	Chromosome + plasmid	MGE

[a]ND, not detected; MGE, mobile genetic element; PCN, plasmid copy number; NA, not applicable.

[b]Outer membrane porin mutations for frameshifts and insertions/deletions notated in amino acid mutation nomenclature. Otherwise, insertion sequence (IS) disruptions are noted in nucleotide space. IS notated with "bp + 1 ATG" indicate IS insertions upstream of the outer membrane porin (*omp*) gene in the promoter region.

[c]β-lactamase genes without preceding insertion sequence and NOT in the same mobilization unit (delimited by "/") do not have sufficient genomic context for MGE estimate. **,Cannot differentiate copy number variants from homologs (i.e., genes with > 95% identity).

[d]Amp. Pred. = amplification prediction. Plasmid copy number contributions were based on normalized coverage depths of full-length plasmid harboring β-lactamase = 1.5×, which indicates approximately 50% of the population has 2 copies of the β-lactamase positive plasmid.

[e]Incomplete and/or short-read assemblies only preclude an estimate of genomic context of β-lactamase gene amplification.

complete genomes available, we found the majority of CNS*Ec* (21/27; 78%) and CNS*Kp* (12/15; 80%) had MGE *in situ* tandem or *ex situ* segmental duplication associated with the increased β-lactamase copy numbers (Table 1 and 2, respectively). Furthermore, with rare exception, these β-lactamase amplifications were associated with observed insertion sequences IS*26* and/or IS*Ecp1* within the CNSE genomes (Table 1 and 2). Stratifying by species and using nomenclature established for these aforementioned MGEs (29), for the 21 CNS*Ec* with MGE mediated β-lactamase gene amplification, 11 (52%) had IS*26* TUs, 8 (38%) had IS*Ecp1* TPUs, and one isolate had both mechanisms (Table 1). Conversely, of the 12 CNS*Kp* with at least two copies of β-lactamase-encoding genes driven by MGEs, eight (67%) had TPUs, three had (25%) TUs, and one isolate had both mechanisms (Table 2). Thus, IS*26*-mediated TU or IS*Ecp1*-mediated TPU amplifications were primarily associated with MGE inter- and intramolecular mobilization of β-lactamases that contributed to carbapenem nonsusceptibility.

When considering the most commonly observed β-lactamase amplifications, we often detected the syntenic coupling on MGEs of $bla_{\text{OXA-1}}$ and/or $bla_{\text{CTX-M-15}}$ with frequent gene amplification either through a TPU or TU structure in CNS*Ec* (11/27; 41%) or CNS*Kp* (8/15;53%) as presented in Table 1 and 2, respectively. Indeed, when measuring binary presence/absence of β-lactamase genes in the entire CNSE cohort, 41% (32/79) of CNSE had $bla_{\text{CTX-M-15}}$/$bla_{\text{OXA-1}}$ cocarriage with both chromosomal and/or plasmid contexts, which is a comparable proportion to what has previously been reported in *E. coli* (38, 39). Of the 31 CNSE isolates that had ONT data available and $bla_{\text{CTX-M-15}}$/$bla_{\text{OXA-1}}$ cocarriage (one of the $bla_{\text{CTX-M-15}}$/$bla_{\text{OXA-1}}$-positive isolates only had a draft assembly), six isolates (three *E. coli* and three *K. pneumoniae*) had the two genes colocalized solely on the chromosome. The majority of $bla_{\text{CTX-M-15}}$/$bla_{\text{OXA-1}}$ colocalization was observed in a plasmid context (81%; 25/31) with all but one CNSE isolate (MB5646) having cocarriage on multireplicon IncF-type plasmids. Therefore, we calculated an estimate of pairwise average nucleotide identity (ANI) of all IncF-type plasmids harboring $bla_{\text{CTX-M-15}}$/$bla_{\text{OXA-1}}$ (Fig. 4) to determine the relatedness of these IncF-type plasmids and see if there was evidence of interclade and interspecies transmission. A full-length visualization of the multireplicon IncF-type plasmids can be found on Fig. S3.

The ANI of all $bla_{\text{CTX-M-15}}$/$bla_{\text{OXA-1}}$-positive IncF-type plasmids was highly similar (average = 0.94; SD = 0.04) across *E. coli* (n = 12) and *Klebsiella* spp. (n = 13) with two primary clusters that formed by species when observing the neighbor joining distance inferred dendrogram (Fig. 4). The discrimination between *E. coli* and *K. pneumoniae* IncFIB plasmids was largely due to differences in transmission of well-characterized replication initiation protein alleles found in *Klebsiella* spp. (i.e., IncFIB$_{\text{K}}$) and *E. coli* (i.e., IncFIB [AP001918]). One nested cluster of five IncFIB plasmids demarcated by a red box in Fig. 4 shared >99.9% ANI across three unique *K. pneumoniae* STs (pMB7868_1, pMB7964_1, and pMB6795_1), *K. aerogenes* (pMB5971_1), and *K. michiganensis* (pMB8590_1). Interestingly, we observed $bla_{\text{CTX-M-15}}$ and/or $bla_{\text{OXA-1}}$ amplification occurring on 8/25 (32%) plasmids (Fig. 4; black striped boxes) with all but one plasmid (pMB2966_1) having an IS*26*-mediated TU amplification. Out of the seven TUs with TU amplification, six were tandem arrays, whereas only one plasmid (pMB8590_1) had a segmental duplication (i.e., mobilization to another genomic context) (Fig. 4).

We next sought to characterize and distinguish the IS*26*- and IS*Ecp1*-mediated mechanisms that were responsible for mobilizing $bla_{\text{CTX-M-15}}$/$bla_{\text{OXA-1}}$ from both a plasmid and chromosomal context. Fig. 5A provides an illustration of a pseudocompound transposon (PCT) that can be made of two or more IS*26* units, which must include flanking IS*26* transposase in direct orientation for potential cointegrate formation to occur and mobilize the passenger AMR genes (40). Fig. 5B shows the highly modular mosaic structures of these PCTs, except for one PCT (MB2910_PCT), include an IS*26* or IS*26*-v1 element upstream of $bla_{\text{CTX-M-15}}$, disrupting the IS*Ecp1* ORF. Interestingly, these PCTs with disrupted IS*Ecp1* were more commonly observed in *E. coli* than in *K. pneumoniae*, apart from five ST307 *K. pneumoniae* isolates (Fig. 5B). There was only one isolate (MB2489) with a likely chromosome-

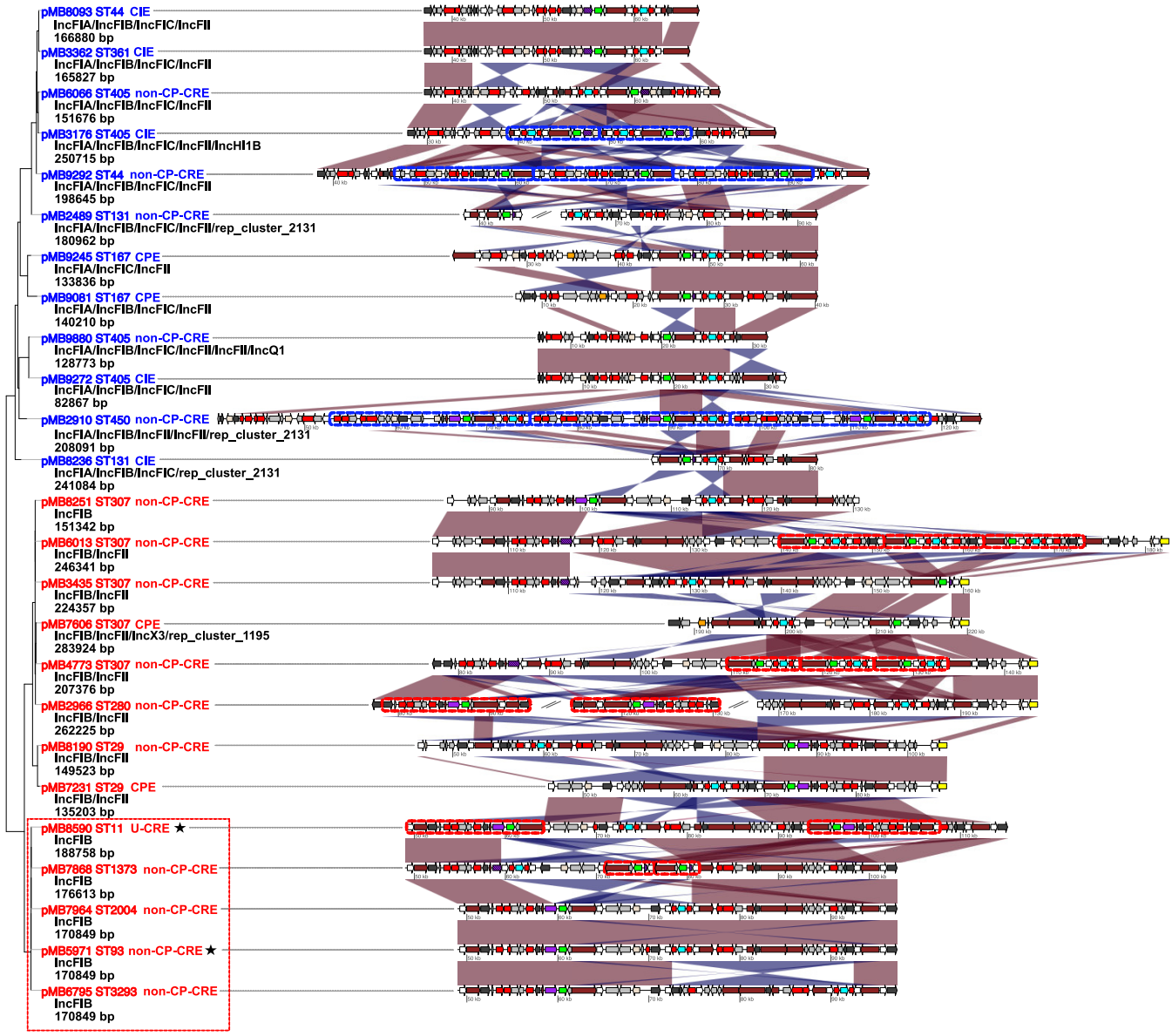

FIG 4 Multireplicon IncF-type plasmids cocarrying $bla_{CTX\text{-}M\text{-}15}$ and $bla_{OXA\text{-}1}$ shared across multiple *Enterobacterales* species. Neighbor-joining (NJ) tree based on estimated ANI pairwise distances of full-length, IncF-type multireplicon plasmids with red tip labels indicating *Klebsiella* spp. and blue tip labels indicating *E. coli* plasmids. Mobilization (MOB) typing designations with plasmid size are beneath each respective NJ tree tip label. Mobile genetic elements that have duplicated are demarcated on sequences with dotted lines colored by species (blue = *E. coli*; red = *K. pneumoniae spp*). Regions of plasmid are subset from each respective plasmid with position indicated on each structure to highlight the multidrug resistance region that includes $bla_{OXA\text{-}1}$ (blue) and $bla_{CTX\text{-}M\text{-}15}$ (green) open reading frame labels. Transposase/integrase (dark gray), IS*26* transposase (white), IS*26*-v1 (off-white), IS*Ecp1* transposase (purple), Tn3-like elements (brown), carbapenemases (orange), other antimicrobial genes (red), *rep* genes (yellow), and other genes (light gray) are labeled accordingly. Striped, purple IS*Ecp1* transposase ORFs indicate a disruption due to IS*26* or IS*26*-v1. The region on NJ tree enclosed by dotted red squares share ~99% identity and with three plasmids (pMB7964, pMB5971, and pMB6796) having ~99% coverage. Stars adjacent to tip labels indicate non-*K. pneumoniae* species (pMB5971 = *K. aerogenes*; pMB8590 = *K. michiganensis*). Linear comparisons between sequences indicate homology shared (min length = 1,000 bp, and >90% identity) in direct (red) and reverse (blue) orientation.

to-plasmid IS*26* transposase-mediated cointegration formation event (Fig. 5B) based on chromosomal gene content present on the plasmid (41, 42).

The other common MGE with the potential to mobilize $bla_{CTX\text{-}M\text{-}15}$/$bla_{OXA\text{-}1}$ was IS*Ecp1*-mediated transposable units (TPUs). Indeed, Fig. 6A provides a schematic for a representative *K. pneumoniae* TPU (MB7231_TPU) found in a chromosomal context. In contrast to CNS*Ec*, 53% of FIB *Klebsiella* spp. plasmids had intact IS*Ecp1* immediately upstream of $bla_{CTX\text{-}M\text{-}15}$ suggesting the potential for TPU formations as the primary driver of $bla_{CTX\text{-}M\text{-}15}$ mobilization in non-ST307 CNS*Kp* (Fig. 6B). There were three CNS*Kp* isolates that had plasmid-to-chromosome transfer of IS*Ecp1*-mediated TPUs, as

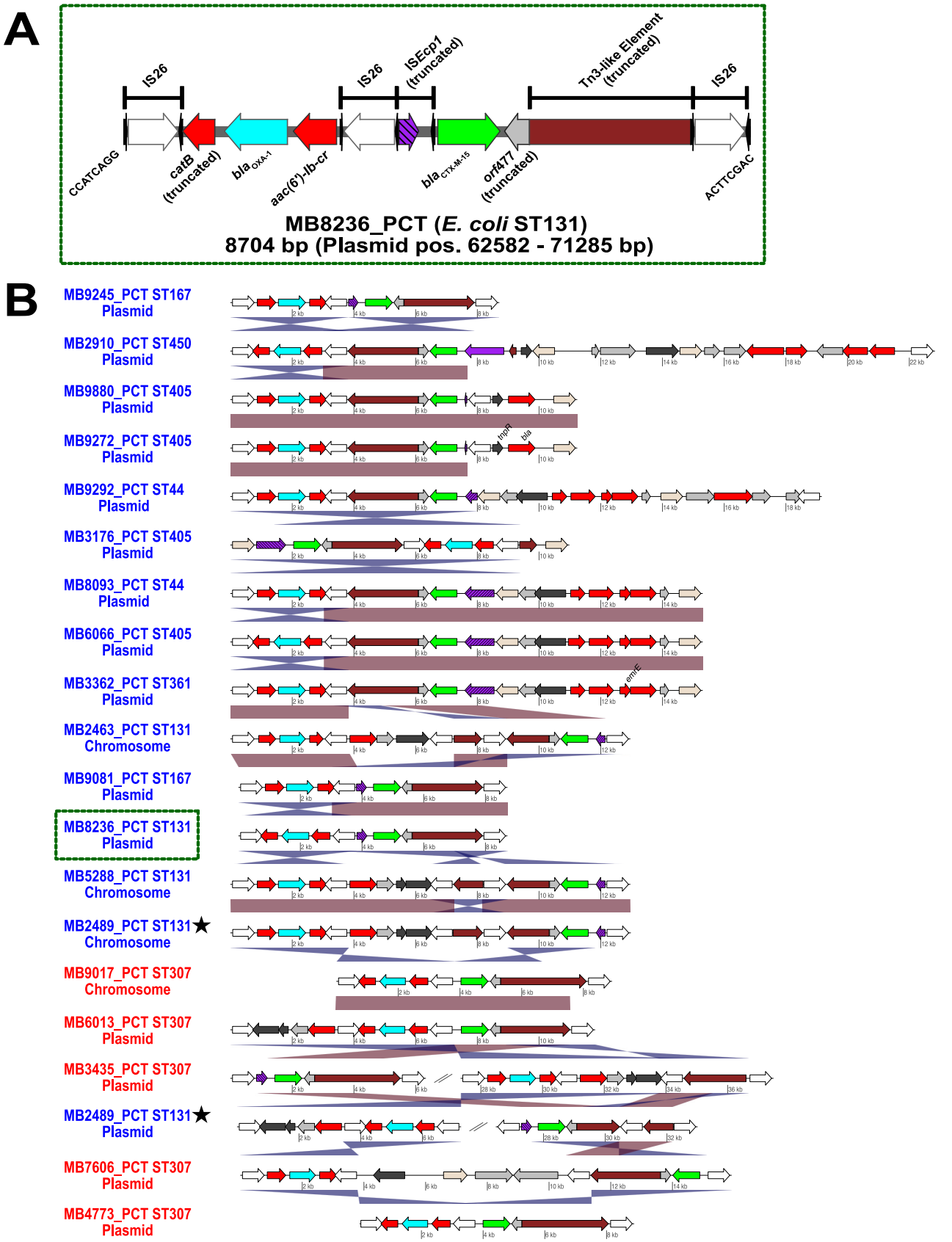

FIG 5 Pseudocompound transposons (PCTs) driving mobilization and amplification of ESBL and narrow-spectrum β-lactamases. Transposase/integrase (dark gray), IS*26* transposase (white), IS*26*-v1 (off-white), IS*Ecp1* transposase (purple), Tn3-like elements (brown), other antimicrobial genes

(Continued on next page)

detected by 5 bp target site duplications flanking the inverted repeat regions of the chromosomal TPUs (Fig. 6B). Taken together, our analysis highlights the enrichment of IS*26*/IS*Ecp1* structures present in CNSE that have a strong association with amplifications of β-lactamase genes, in particular, $bla_{\text{CTX-M-15}}$ and $bla_{\text{OXA-1}}$ in our cohort.

Characterization of unconfirmed nonsusceptible *Enterobacterales* (U-CNSE) isolates. In light of the increasing recognition of the impact of unconfirmed CRE (1), we next sought to characterize a subset of *E. coli* and *Klebsiella* spp. for which we had not confirmed carbapenem nonsusceptibility to our non-CP-CNSE isolates. In marked contrast to non-CP-CR*Ec* and non-CP-CR*Kp* isolates, none of the U-CNS *E. coli* (n = 3) and *Klebsiella* spp. (n = 2) had mutated OmpC/OmpF (OmpK36/OmpK35)-encoding genes (Fig. 2; Table S2). All the U-CNS *E. coli* and *Klebsiella* spp. were $bla_{\text{CTX-M}}$-positive (4 $bla_{\text{CTX-M-15}}$; 1 $bla_{\text{CTX-M-55}}$); furthermore, amplification of ESBL encoding enzymes were detected (median ESBL CNV = 2.4×) among all five. U-CNS *E. coli* and *Klebsiella* spp. β-lactamase gene amplification in the U-CNS isolates shared similar mechanisms to that observed for the non-CP-CRE strains. For example, MB8590 (*K. michiganensis*; ST11) had evidence of a plasmid TU harboring $bla_{\text{CTX-M-15}}$/$bla_{\text{OXA-1}}$ that had two copies via segmental duplication (Fig. 4). Furthermore, this TU included an intact IS*Ecp1* (Fig. 6B) suggesting the potential for TPU-mediated mobilization as well. Although a small number of isolates were examined, these data indicate that intact porins are the major distinction between unconfirmed and CNS *E. coli* and *Klebsiella* spp.

DISCUSSION

Through a comprehensive, comparative genomics analysis on a diverse array of CNSE bacteremia isolates, we expanded the current understanding of the breadth of MGE-mediated mechanisms used to overcome carbapenems in clinically important *Enterobacterales* strains. By analyzing normalized coverage depths of β-lactamase-encoding genes in conjunction with the detection of binary presence/absence of β-lactamases and *omp* genes, we show that amplification of ESBL genes as well as disruption of *omp* genes are commonly found among invasive non-CP-CRE. Additionally, our ONT long-read sequencing data allowed for full characterization of the complex MGE-mediated gene amplifications and genetic alterations that can generate carbapenem resistance in the absence of a carbapenemase. The increasing appreciation of both the scope and clinical impact of non-CP-CRE (1, 2) highlights the need to develop novel diagnostic and therapeutic strategies for this understudied group of organisms.

A key finding was the high prevalence of CNSE organisms that lacked carbapenemases with non-CP strains accounting for well over 70% of both CNS *E. coli* and *K. pneumoniae* in our cohort. One possible explanation for this finding was our inclusion of organisms with carbapenem-intermediate susceptibility phenotypes (i.e., CIE strains), a decision which was based on the recent CRACKLE-2 finding that patients with unconfirmed CNSE, which often tested intermediate to ertapenem or other carbapenems, had similar clinical outcomes to patients with confirmed CRE (1). Given that carbapenem MICs tend to be lower for non-CP-CRE versus CPE (1, 34, 43), our inclusion of CIE strains likely increased our proportion of non-CP isolates. However, even when only CRE isolates were considered, we still observed a predominance of non-CP organisms for both *E. coli* (19/25; 76%) and *K. pneumoniae* (18/26; 69%). Whereas a high percentage of non-CP-CR*Ec* strains has consistently been found in CRE surveillance studies, the opposite is true of *K. pneumoniae* where the high prevalence of bla_{KPC} typically results in >70 to 80% of CR*Kp* organisms being carbapenemase-positive in the United States (1, 34). The high percentage of non-CP-CRE in our cohort was

FIG 5 Legend (Continued)
(red), $bla_{\text{OXA-1}}$ (blue), $bla_{\text{CTX-M-15}}$ (green), and other genes (light gray) are labeled accordingly. Striped, purple IS*Ecp1* transposase ORFs indicate a disruption due to IS*26* or IS*26*-v1. (A) Representation of pseudocompound transposon (MB8236_PCT) flanked by IS*26* in direct orientation within a plasmid context. Black arrows flanking IS transposases indicate inverted repeats. There is an 8-bp DNA flanking IS*26* on linearized representation of PCT. Position on plasmid is indicated in parenthesis. (B) Plasmid and chromosomal contexts of PCT within *E. coli* (blue) and *K. pneumoniae* (red) indicating blastn identities as described in Fig. 4. Stars indicate PCTs arising from the same genome. Green dotted line highlights the PCT that is fully annotated in (A). Linear comparisons between sequences indicate homology shared (min length = 1,000 bp, and >90% identity) in direct (red) and reverse (blue) orientation.

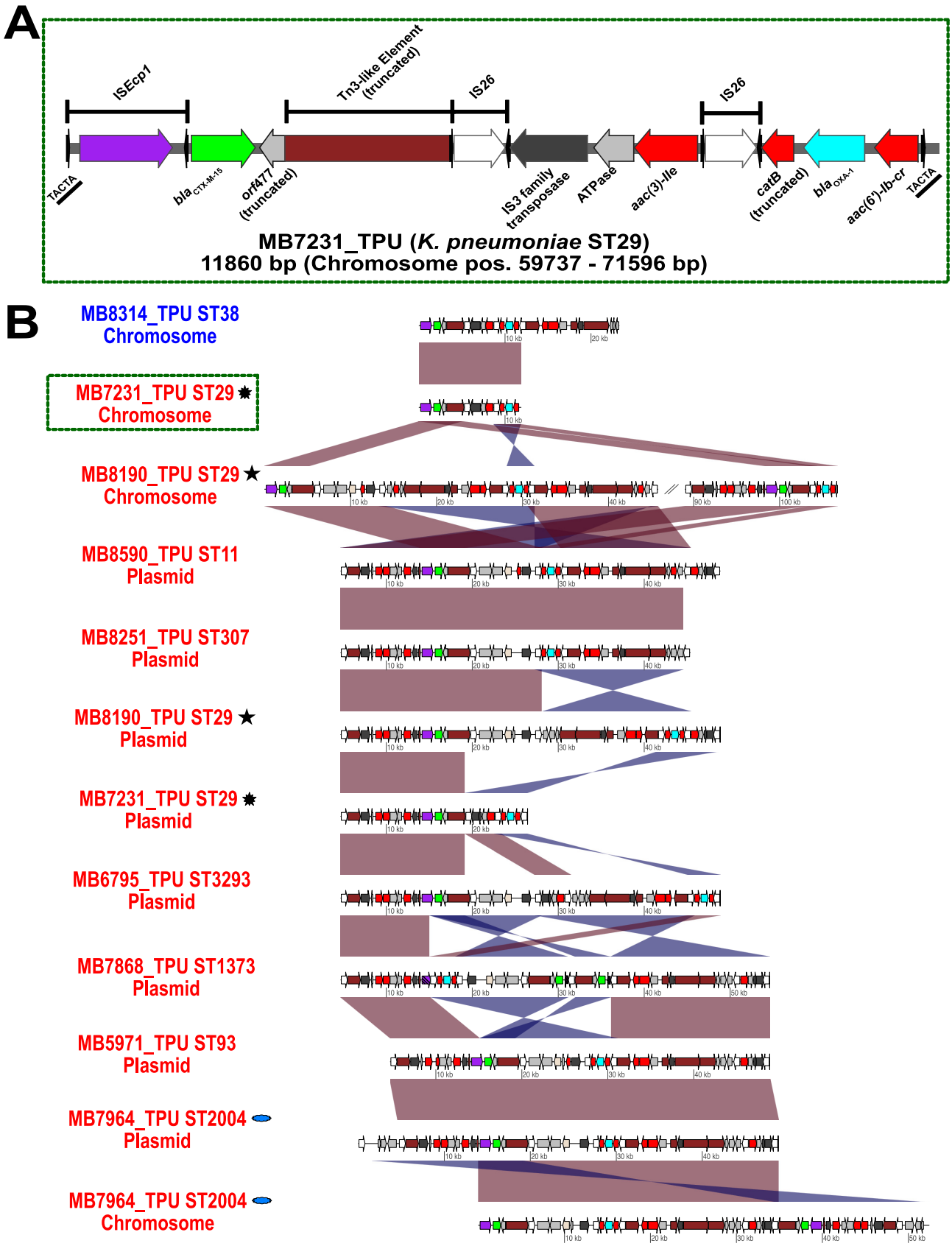

FIG 6 Transposition units (TPUs) driving mobilization and amplification of ESBL and narrow-spectrum β-lactamases. Transposase/integrase (dark gray), IS*26* transposase (white), IS*26*-v1 (off-white), IS*Ecp1* transposase (purple), Tn*3*-like elements (brown), other antimicrobial genes (red), bla_{OXA-1}

(Continued on next page)

particularly interesting given that we only examined bacteremia isolates which are sufficiently fit to cause a serious infection inasmuch as non-CP-CRE isolates are often considered to have a fitness defect relative to CPE strains (44–46). The reasons underlying the high prevalence of non-CP isolates in our bacteremia cohort are not currently known but may include relatively stringent infection control practices among our highly immunocompromised patients. Recently, Black et al. noted a higher prevalence of non-CP-CRE (59%) in south Texas where non-CP-CRE patients were more likely to receive a longer duration of antibiotic treatment as well as more likely to have an emergency department visit compared to CPE, albeit with low number of observations (47). This finding is consistent with our cancer patient population that receives a high level of antibiotic treatment (48) and coincides with the finding that previous antibiotic exposure has been identified as a risk factor for non-CP-CRE relative to CPE in other studies (7).

The high percentage of non-CP organisms in our cohort led us to focus on using our genomic data to better understand mechanisms driving carbapenem resistance in the absence of a carbapenemase. There were several important findings from these analyses. First, consistent with previous data based primarily on laboratory studies of passaged strains and PCR-based methods (24–26), we found that non-CP-CRE almost always had combined porin disruption and amplification of ESBL-encoding genes. While many studies have documented how an increase in AMR gene copy number corresponds to an increased AMR phenotype (13–17, 33), to our knowledge, our study is the first to systematically demonstrate an ESBL gene copy number increase in a large cohort of non-CP-CRE bacteremia isolates. It is thought that the porin disruption limits carbapenem penetration into the periplasm to the point where high level ESBL production can inactivate sufficient carbapenem to generate resistance (4). Thus, incorporating porin assessment and β-lactamase gene amplification could assist with predicting *Enterobacterales* carbapenem susceptibility using genomic data (49–51). Second, the non-CP-CRE isolates were genetically heterogenous and primarily encoded various CTX-M-type ESBLs with or without OXA-1. ESBL variants of TEM or SHV were quite rare in *E. coli* ($n = 2$) and *K. pneumoniae* ($n = 3$), as was plasmid-borne AmpC in *E. coli* ($n = 5$) and *K. pneumoniae* (not detected). These findings may reflect the dominant nature of CTX-M-containing strains among ESBL isolates and are congruent with a previous laboratory study indicating multiple classes of CTX-M enzymes can reduce ertapenem susceptibility under selective pressure in porin deficient backgrounds (26). Finally, we observed minimal clonality among the non-CP-CRE strains indicating that the organisms developed carbapenem resistance independently rather than being transmitted between patients. This hypothesis is supported by our observation that in many of the non-CP-CR *E. coli* and *K. pneumoniae* cases, the patients had previously had a bloodstream infection with an ESBL-producing carbapenem-susceptible organism. Thus, it is highly likely that carbapenem treatment of the ESBL infection selected for non-CP-CRE strains via ESBL amplification and porin disruption. Given that in our previous study only a small percentage of patients treated for an ESBL infection subsequently developed a non-CP-CRE infection (13), we are actively investigating why particular genetic backgrounds may contribute to a higher probability of developing carbapenem resistance versus other ESBL-positive *Enterobacterales* strains.

The use of ONT sequencing was critical in helping to delineate the diverse MGE mechanisms underlying increases in ESBL gene copy numbers, which in general are not discernible with the commonly used short-read, whole-genome sequencing or PCR-based approaches (19). The vast majority of the ESBL amplifications involved CTX-M encoding genes with long-read data, indicating that these amplifications were likely due to IS*26*

FIG 6 Legend (Continued)
(blue), $bla_{\text{CTX-M-15}}$ (green), and other genes (light gray) are labeled accordingly. Striped, purple IS*Ecp1* transposase ORFs indicate a disruption due to IS*26*. (A) Example of *K. pneumoniae* chromosomal context of transposition unit (MB7231_TPU) mobilized from plasmid to chromosome via IS*Ecp1*. Black arrows flanking IS transposases indicate inverted repeats. A 5-bp direct repeat (underlined) flanking MB7231_TPU is indicated on end of the linearized representation of TPU. Position on chromosome indicated in parenthesis. (B) Plasmid and chromosomal contexts of TPU within *E. coli* (blue) and *K. pneumoniae* (red) indicating blastn identities as described in Fig. 4. Matching symbols adjacent to labels indicate TPUs arising from the same genome. The green dotted line highlights the TPU that is fully annotated in (A). Linear comparisons between sequences indicate homology shared (min length = 1,000 bp, and >90% identity) in direct (red) and reverse (blue) orientation.

translocatable units or IS*Ecp1* transposition units increasing in copy via segmental duplication or *in situ* tandem amplification. Both IS*26* and IS*Ecp1* contain transposases capable of mobilizing AMR genes (albeit very different mechanisms), with IS*26*-mediated gene amplification increasingly recognized as a cause of progressive resistance to various β-lactams (13, 15, 20, 41, 42, 52). The complex MGEs amplified by IS*26* and IS*Ecp1* often contained non-β-lactamase-encoding genes that confer resistance to aminoglycosides (e.g., *aac[6′]-Ib-cr*), tetracyclines (e.g., *tetAR*), trimethroprim (e.g., *dfrA17*), and sulfonamides (e.g., *sul1*) as illustrated in Fig. 4 and 6. Therefore, similar to CPE, our non-CP-CRE was often multidrug resistant (Table S4), further hindering treatment options. Another finding of concern was identifying IS*26* or IS*Ecp1* coamplification of two β-lactamases on the same transposable unit (Table 1 and 2), typically $bla_{\text{CTX-M-15}}$ along with $bla_{\text{OXA-1,}}$ but also $bla_{\text{CTX-M-15}}$ with $bla_{\text{CMY-4}}$ and $bla_{\text{CTX-M-55}}$ with $bla_{\text{CMY-2}}$. These dual β-lactamase-encoding gene amplified organisms often were nonsusceptible to meropenem in addition to ertapenem (Table S4).

Our findings along with other data (30, 31, 51) suggest carbapenem-nonsusceptible *Enterobacterales* reside along a spectrum mediated to a major degree by changes in porin function and β-lactamase gene copy number. It is likely that unconfirmed CNSE consist of a heterogenous population of ESBL-positive, carbapenem-adapting strains with β-lactamase gene amplifications/porin disruptions which may give different phenotypic results depending on the colony tested (32). Further carbapenem adaptation may fix a single porin disruption as seen in our *E. coli* ST405 isolates in Fig. 2, and/or increase β-lactamase gene copy number within the population, leading to a carbapenem-intermediate phenotype that progresses to full resistance through further β-lactamase amplification and concurrent outer membrane porin disruption. This progressive β-lactam resistance model is analogous to that recently identified for $bla_{\text{TEM-1}}$ and $bla_{\text{OXA-1}}$ amplifications mediating piperacillin-tazobactam resistance (13, 15, 16, 33). The increasing rates of ESBL-positive *Enterobacterales* infections means that there are growing opportunities for development of non-CP-CRE. Given the widespread nature of IS*26*-mediated TUs and IS*Ecp1*-mediated TPUs in association with ESBL enzymes, our data suggest that optimizing carbapenem therapy (choice of carbapenem, dose, and duration) of ESBL infections is likely to be critical to minimizing non-CP-CRE emergence.

Our study has some inherent limitations. First, we only assayed strains from a gDNA context. It is likely that non-CP-CRE mechanisms also include transcriptional and post-transcriptional changes that we did not discern. However, there were only a few CNSE strains where a DNA-based explanation for an observed phenotype could not be identified, and these strains will be assessed using other methodologies as part of future studies. Second, we focused on particular genomic areas, specifically, known β-lactamase-encoding elements and porin-encoding genes. Thus, it remains possible that other, yet to be identified, DNA alterations contributed to the carbapenem susceptibility phenotypes. Similarly, we did not recreate the DNA modifications of interest in an isogenic background to conclusively demonstrate that the identified changes conferred carbapenem resistance. However, our findings are in line with those derived from previous laboratory passaged and genetically altered strains (24–26). Finally, given the large number of sequenced isolates, we did not assess for population heterogeneity, the impact of which we attempted to minimize by performing phenotypic and genotypic analyses on the same single colony.

In summary, we present a cohort of fully resolved genomes of carbapenem-nonsusceptible *Enterobacterales* causing invasive infections, focusing on a large number of noncarbapenemase-producing *E. coli* and *K. pneumoniae* isolates. Our data shed light on the pleiotropic and potentially widespread mechanisms underlying the non-CP-CRE phenotype and suggest that antimicrobial stewardship practices are likely to be critical in efforts to decrease non-CP-CRE impact.

MATERIALS AND METHODS

Study design. Our lab has a comprehensive storage of The University of Texas MD Anderson Cancer Center (MDACC) bacteremia isolates (i.e., the Microbe Bank Database [MBD]) dating back to 2012 stocked at −80°C in thioglycolate media with 25% glycerol. CLSI 2018 M100 guidelines were used to determine MIC breakpoint interpretations for carbapenem resistance (53). *Enterobacterales* bacteremia

isolates (n = 143) with a nonsusceptible MIC interpretation to ertapenem (ETP) (>0.5 μg/mL) or meropenem (MEM) (>1 μg/mL) as reported by the MDACC Division of Pathology and Laboratory Medicine (PLM) clinical microbiology laboratory were selected using the Epic EHR software workbench reporting tool from July 1st, 2016, to June 30th, 2020. *Enterobacterales* species with intrinsic resistance to carbapenems (e.g., *Proteus mirabilis*) were excluded from selection. Candidate isolates underwent additional MIC testing to confirm ETP nonsusceptibility as identified by the PLM lab using Etest (bioMérieux) gradient MIC strips. Definitions of carbapenem nonsusceptibility were based on the following criterion: (1) carbapenemase-producing *Enterobacterales* (CPE) = carbapenemase detection confirmed through whole-genome sequencing (WGS); (2) noncarbapenemase-producing carbapenem-resistant *Enterobacterales* (non-CP-CRE) = no carbapenemase detected in WGS with confirmation Etest ETP MIC $\geq$ 2 μg/mL *and* MDACC ETP MIC $\geq$ 2 μg/mL, *or* MEM MIC $\geq$ 4 μg/mL; (3) carbapenem intermediate *Enterobacterales* (CIE) = (a) confirmation Etest 0.5 μg/mL < ETP MIC < 2.0 μg/mL, or (b) MDACC MIC where 0.5 μg/mL < ETP MIC < 2.0 μg/mL *or* 1 μg/mL < MEM MIC < 4.0 μg/mL; (4) unconfirmed carbapenem nonsusceptible *Enterobacterales* (U-CNSE) = confirmation Etest ETP MIC $\leq$ 0.5 μg/mL.

CNSE exclusion criteria included isolates not available in the MBD (n = 10), serial isolates (i.e., any consecutive, recurrent bacteremia isolate with identical species as identified by the PLM lab) (n = 25), isolates from same culture (n = 4), and U-CNSE phenotype isolates and/or isolates with no growth on ertapenem (0.5 μg/mL) supplemented THY agar (n = 25). The first available ETP-nonsusceptible isolate per patient from the MBD that met the above definition and the screening process, was selected for whole-genome sequencing. There were two isolates, MB8134 and MB8251, with differential *Enterobacterales* species cultured from the same patient and isolated 18 days apart, that were included in the total CNSE cohort. After screening for carbapenem nonsusceptibility from available isolates (see Fig. 1), our sampling frame resulted in 79 total CNSE isolates that were sequenced from 78 unique patients. In addition to our CNSE WGS cohort, we performed WGS on 8 U-CNSE to investigate unstable carbapenem-nonsusceptible phenotypes. An antibiogram of the 79 CNSE isolates + 8 U-CNSE isolates is available on Table S4.

Illumina short-read and Oxford Nanopore Technologies long-read sequencing. All isolates were streaked from the MBD collection and grown on THY overnight at 37°C. Single colonies were picked and grown in LB broth for 4 h at 37°C with mild agitation and subsequently a pellet was stored at −80°C until gDNA extraction. The extraction of gDNA was performed using the MasterPure Complete DNA and RNA purification kit using manufacturer's instructions. Genomic DNA concentration was measured using the Qubit 4 fluorometer with complementary measurement of concentration and A260/280; A260/230 performed on an Eppendorf BioPhotometer. Isolates were then library prepped using the Illumina DNA Prep kit and sequenced using the Illumina NovaSeq 6000 platform. Select isolates were then sequenced using the long-read Oxford Nanopore Technologies (ONT) GridION platform with the Rapid Sequencing kit (SQK-RAD004) per manufacturer's instructions.

Short-read Illumina fastq data were trimmed, quality checked, and assembled using a customized workflow (Shropshire W, SPAdes_pipeline-v0.1.0-alpha, GitHub: https://github.com/wshropshire/SPAdes_pipeline) with assemblies generated using SPAdes v3.15.3 using the "—isolate" parameter in addition to default parameters for paired-end short-read data. Short-read and long-read data were used with the Flye v2.9-b1768 assembler pipeline (Shropshire, W.; flye_hybrid_assembly_pipeline-v0.3.0-alpha; https://github.com/wshropshire/flye_hybrid_assembly_pipeline). Genome assembly quality was assessed with CheckM v1.2.0 (54) with mean coverage depth of complete and draft assemblies calculated using mosdepth v0.3.3 (55). An overview of genome assembly quality metrics is presented on Table S6.

Pan genome and maximum likelihood (ML) phylogenetic analysis. Complete and draft assemblies were then used as input for pan genome analysis using Panaroo v.1.2.9 (56) using the moderate --clean-mode parameter with the mafft core gene alignment option. This core gene alignment file was then used as input to create a maximum-likelihood phylogenetic tree with IQTree2 v2.2.0-beta (57). When creating the core gene inferred ML phylogenetic tree, model selection was performed using ModelFinder (58), a nonparametric bootstrap approximation, UFBoot (59) (n = 1,000), and an SH-aLRT (n = 1,000) test to further evaluate branch lengths. Tree visualization along with the addition of metadata was completed using ggtree v3.1.1 and ggtreeExtra v1.0.4, respectively. Clustering of isolates based on core gene alignment was assessed using the rhierhaps-1.1.3 tool (60). Pairwise SNP differences were assessed using the snp-dists tool (Seemann, T.; snp-dists-v0.8.2; https://github.com/tseemann/snp-dists).

Antimicrobial resistance genes and *in silico* typing profiles. Kleborate v2.0.4 (61) was used with draft and complete assemblies to identify K and O antigen profiles (Kleborate confidence scores of "Good" or better), MLST, acquired and chromosomal antimicrobial resistance, and virulence factors for isolates belonging to the *Klebsiella pneumoniae* species complex (KpSC). Additionally, Kleborate (61) was used to designate species taxa for all isolates sequenced by calculating pairwise Mash distances (62) between each respective genome assembly and their Enterobacterales reference genomes (n = 2,619). All isolates had strong species matches (i.e., Mash distances < 0.02). SerotypeFinder v2.0 (63) was used for *in silico* serotyping of *E. coli* isolates using an 85% blastn identity/60% minimum length threshold for O and H antigen identification using complete or draft assemblies. Novel MLST schema not identified using Kleborate v2.0.4 or the mlst v2.19.0 Perl script (Seemann, T.; mlst-2.19.0; https://github.com/tseemann/mlst) was identified using the MLST v2.0 server (64). Phylogroups of *E. coli* were detected using the ClermonTyping v20.03 tool (65) using the clermonTyping.sh script. The BLASTn alignment tool (BLAST 2.11.0+) was used with an in-house database of *E. coli ompC* and *ompF* genes (MG1655 K-12 reference) and their respective enterobacterial homologs identified in *Klebsiella* spp., *Enterobacter* spp., *Citrobacter* spp., and *Serratia marcescens* to characterize potential osmoporin gene disruption. SnapGene v5.0.8 was used to visualize these osmoporin gene disruptions and further characterize MGE-associated insertions within the open reading frame and/or promoter region using ISFinder (66).

AMR gene and plasmid copy number variation estimation. Antimicrobial resistance genes were detected using the KmerResistance v2.2.0 (67, 68) tool which uses KMA-1.3.24a to detect AMR genes using a short-read k-mer-based alignment against the ResFinder (Accessed 5 November 2021). These ResFinder hits were then used as input for a copy number variant estimation tool (Shropshire, W.; convict-v1.0; https://github.com/wshropshire/convict), which estimates gene copy number variants by normalizing coverage depths to housekeeping genes. Core genes present in >99% of the consensus, pan genome fasta file generated from Panaroo were used to control coverage depth (i.e., 3211 core genes). We only reported AMR gene copy number variants with 100% coverage and 100% identity as reported through KmerResistance. We performed qPCR for further validation of CONVICT with one high and low CNV $bla_{CTX\text{-}M\text{-}15}$/$bla_{OXA\text{-}1}$ sample (MB5288 and MB8093, respectively) with results presented on Fig. S4.

SVants (Hanson, B.; GitHub: https://github.com/EpiBlake/SVants) was used to confirm copy number variants with individual ONT long-reads containing multiple tandem repeats of IS*26* and IS*Ecp1* multiresistance determinant regions for isolates with increased coverage depth mapping visualized in IGV-2.9.4. A ratio of mean coverage depths of plasmid-to-chromosome was calculated using bwa mem alignments and the pileup.sh script from bbmap-v38.79 to get an approximation of plasmid copy number (PCN).

Plasmid typing of completed assemblies was completed using the mob_typer-v3.0.0 command line tool (69). FastANI-v1.31 (70) was used to estimate average nucleotide identity across plasmid and MGE structures with default settings. The bacsort script (Wick, R.; GitHub: https://github.com/rrwick/Bacsort), "pairwise_identities_to_distance_matrix.py" is used to convert FastANI pairwise distances to a distance matrix in PHYLIP format with a maximum genetic distance of 0.20. This distance matrix was used as input to create a neighbor-joining tree using the BIONJ algorithm (71) using the ape-v.5.6-1 R package (72). Genome comparisons and annotations of plasmid and MGE structures was performed using the genoPlotR-v0.8.11 R package (73). In order to filter multiple IS comparisons, a minimum sequence fragment length of 1000 bp was used to compare blastn identities ≥90% in direct (red) or reverse (blue) orientation.

Statistics. All statistics were performed using R v4.0.4 (15 February 2021). Significant increases in AMR gene copy numbers were assessed using one-sample Wilcoxon tests with a one-sided alternative hypothesis that mean CNV was greater than 1. Scatterplot and boxplots were generated using ggplot2 v3.3.5.

Data availability. Short-read Illumina data, long-read ONT data, as well as complete and draft assemblies are available in the NCBI BioProject repository (PRJNA836696). Three samples (MB2315, MB2446, MB2463) have data available from a previous BioProject (PRJNA603908).

SUPPLEMENTAL MATERIAL

Supplemental material is available online only.

FIG S1, EPS file, 0.1 MB.
FIG S2, EPS file, 0.2 MB.
FIG S3, PDF file, 0.6 MB.
FIG S4, EPS file, 0.9 MB.
TABLE S1, XLSX file, 0.01 MB.
TABLE S2, XLSX file, 0.02 MB.
TABLE S3, XLSX file, 0.01 MB.
TABLE S4, XLSX file, 0.02 MB.
TABLE S5, XLSX file, 0.01 MB.
TABLE S6, XLSX file, 0.02 MB.

ACKNOWLEDGMENTS

Illumina short-read sequencing was done through the MDACC Advanced Technology Core (ATGC) using core grant CA016672 (ATGC) with the Illumina NovaSeq6000 (NIH 1S10OD024977-01). Support for this study was provided by the National Institute of Allergy and Infectious Diseases (NIAID) R21AI151536 and P01AI152999 for S.A.S. NIAID K24AI121296, R01AI134637, R01AI148342, and P01AI152999 supported C.A.A. B.M.H. was supported by the NIAID K01AI148593. The research in the A.K. laboratory is supported by NIGMS 1R01GM133904-01 and the Welch Foundation Research Grant AU-1998-20190330.

REFERENCES

1. van Duin D, Arias CA, Komarow L, Chen L, Hanson BM, Weston G, Cober E, Garner OB, Jacob JT, Satlin MJ, Fries BC, Garcia-Diaz J, Doi Y, Dhar S, Kaye KS, Earley M, Hujer AM, Hujer KM, Domitrovic TN, Shropshire WC, Dinh A, Manca C, Luterbach CL, Wang M, Paterson DL, Banerjee R, Patel R, Evans S, Hill C, Arias R, Chambers HF, Fowler VG, Kreiswirth BN, Bonomo RA, Multi-Drug Resistant Organism Network Investigators. 2020. Molecular and clinical epidemiology of carbapenem-resistant Enterobacterales in the USA (CRACKLE-2): a prospective cohort study. Lancet Infectious Diseases 20:731–741. https://doi.org/10.1016/S1473-3099(19)30755-8.
2. Guh AY, Bulens SN, Mu Y, Jacob JT, Reno J, Scott J, Wilson LE, Vaeth E, Lynfield R, Shaw KM, Vagnone PM, Bamberg WM, Janelle SJ, Dumyati G, Concannon C, Beldavs Z, Cunningham M, Cassidy PM, Phipps EC, Kenslow N, Travis T, Lonsway D, Rasheed JK, Limbago BM, Kallen AJ. 2015. Epidemiology of carbapenem-resistant Enterobacteriaceae in 7 US communities, 2012-2013. JAMA 314:1479–1487. https://doi.org/10.1001/jama.2015.12480.

3. Dagher C, Salloum T, Alousi S, Arabaghian H, Araj GF, Tokajian S. 2018. Molecular characterization of Carbapenem resistant Escherichia coli recovered from a tertiary hospital in Lebanon. PLoS One 13:e0203323. https://doi.org/10.1371/journal.pone.0203323.
4. Nordmann P, Poirel L. 2019. Epidemiology and diagnostics of carbapenem resistance in Gram-negative bacteria. Clin Infect Dis 69:S521–S528. https://doi.org/10.1093/cid/ciz824.
5. Satlin MJ, Jenkins SG, Walsh TJ. 2014. The global challenge of carbapenem-resistant Enterobacteriaceae in transplant recipients and patients with hematologic malignancies. Clin Infect Dis 58:1274–1283. https://doi.org/10.1093/cid/ciu052.
6. Nguyen MH, Shields RK, Chen L, Pasculle AW, Hao B, Cheng S, Sun J, Kline EG, Kreiswirth BN, Clancy CJ. 2022. Molecular epidemiology, natural history and long-term outcomes of multi-drug resistant Enterobacterales colonization and infections among solid organ transplant recipients. Clinical Infectious Diseases 74:395–406. https://doi.org/10.1093/cid/ciab427.
7. Marimuthu K, Ng OT, Cherng BPZ, Fong RKC, Pada SK, De PP, Ooi ST, Smitasin N, Thoon KC, Krishnan PU, Ang MLT, Chan DSG, Kwa ALH, Deepak RN, Chan YK, Chan YFZ, Huan X, Zaw Linn K, Tee NWS, Tan TY, Koh TH, Lin RTP, Hsu LY, Sengupta S, Paterson DL, Perencevich E, Harbarth S, Teo J, Venkatachalam I, Cherng B, Su Gin DC, Rama Narayana D, De PP, Li Yang H, Venkatachalam I, Teo J, Marimuthu K, Tse Hsien K, Tee N, Smitasin N, Oon Tek N, Say Tat O, Krishnan PU, Fong R, Lin Tzer Pin R, Pada SK, Thean Yen T, Koh Cheng T, for the CaPES Study Group. 2019. Antecedent carbapenem exposure as a risk factor for non-carbapenemase-producing carbapenem-resistant Enterobacteriaceae and carbapenemase-producing Enterobacteriaceae. Antimicrob Agents Chemother 63 https://doi.org/10.1128/AAC.00845-19.
8. Bouganim R, Dykman L, Fakeh O, Motro Y, Oren R, Daniel C, Lazarovitch T, Zaidenstein R, Moran-Gilad J, Marchaim D. 2020. The clinical and molecular epidemiology of noncarbapenemase-producing carbapenem-resistant Enterobacteriaceae: a case-case-control matched analysis. Open Forum Infect Dis 7:ofaa299. https://doi.org/10.1093/ofid/ofaa299.
9. Shropshire WC, Dinh AQ, Earley M, Komarow L, Panesso D, Rydell K, Gómez-Villegas SI, Miao H, Hill C, Chen L, Patel R, Fries BC, Abbo L, Cober E, Revolinski S, Luterbach CL, Chambers H, Fowler VG, Bonomo RA, Shelburne SA, Kreiswirth BN, Duin Dv, Hanson BM, Arias CA. 2022. Accessory Genomes Drive Independent Spread of Carbapenem-Resistant Klebsiella pneumoniae Clonal Groups 258 and 307 in Houston, TX. mBio 13:e00497-22.
10. Wyres KL, Lam MMC, Holt KE. 2020. Population genomics of Klebsiella pneumoniae. Nat Rev Microbiol 18:344–359. https://doi.org/10.1038/s41579-019-0315-1.
11. Mathers AJ, Peirano G, Pitout JDD. 2015. The role of epidemic resistance plasmids and international high-risk clones in the spread of multidrug-resistant Enterobacteriaceae. Clin Microbiol Rev 28:565–591. https://doi.org/10.1128/CMR.00116-14.
12. Poirel L, Bonnin RA, Nordmann P. 2012. Genetic support and diversity of acquired extended-spectrum β-lactamases in Gram-negative rods. Infect Genet Evol 12:883–893. https://doi.org/10.1016/j.meegid.2012.02.008.
13. Shropshire WC, Aitken SL, Pifer R, Kim J, Bhatti MM, Li X, Kalia A, Galloway-Peña J, Sahasrabhojane P, Arias CA, Greenberg DE, Hanson BM, Shelburne SA. 2021. IS26-mediated amplification of blaOXA-1 and blaCTX-M-15 with concurrent outer membrane porin disruption associated with de novo carbapenem resistance in a recurrent bacteraemia cohort. J Antimicrob Chemother 76:385–395. https://doi.org/10.1093/jac/dkaa447.
14. Hansen KH, Andreasen MR, Pedersen MS, Westh H, Jelsbak L, Schonning K. 2019. Resistance to piperacillin/tazobactam in Escherichia coli resulting from extensive IS26-associated gene amplification of blaTEM-1. J Antimicrob Chemother 74:3179–3183. https://doi.org/10.1093/jac/dkz349.
15. Hubbard ATM, Mason J, Roberts P, Parry CM, Corless C, Van Aartsen J, Howard A, Bulgasim I, Fraser AJ, Adams ER, Roberts AP, Edwards T. 2020. Piperacillin/tazobactam resistance in a clinical isolate of Escherichia coli due to IS26-mediated amplification of blaTEM-1B. Nat Commun 11 https://doi.org/10.1038/s41467-020-18668-2.
16. Schechter LM, Creely DP, Garner CD, Shortridge D, Nguyen H, Chen L, Hanson BM, Sodergren E, Weinstock GM, Dunne WM, van Belkum A, Leopold SR. 2018. Extensive gene amplification as a mechanism for piperacillin-tazobactam resistance in Escherichia coli. mBio 9:e00583-18. https://doi.org/10.1128/mBio.00583-18.
17. Simner PJ, Mostafa HH, Bergman Y, Ante M, Tekle T, Adebayo A, Beisken S, Dzintars K, Tamma PD. 2021. Progressive development of cefiderocol resistance in Escherichia coli during therapy is associated with an increase in blaNDM-5 copy number and gene expression. Clinical Infectious Diseases https://doi.org/10.1093/cid/ciab888.
18. Khan A, Shropshire WC, Hanson B, Dinh AQ, Wanger A, Ostrosky-Zeichner L, Arias CA, Miller WR. 2020. Simultaneous infection with Enterobacteriaceae and Pseudomonas aeruginosa harboring multiple carbapenemases in a returning traveler colonized with Candida auris. Antimicrob Agents Chemother 64. https://doi.org/10.1128/AAC.01466-19.
19. George S, Pankhurst L, Hubbard A, Votintseva A, Stoesser N, Sheppard AE, Mathers A, Norris R, Navickaite I, Eaton C, Iqbal Z, Crook DW, Phan HTT. 2017. Resolving plasmid structures in Enterobacteriaceae using the MinION nanopore sequencer: assessment of MinION and MinION/Illumina hybrid data assembly approaches. Microb Genom 3:e000118. https://doi.org/10.1099/mgen.0.000118.
20. Feng Y, Liu L, McNally A, Zong Z. 2018. Coexistence of two blaNDM-5 genes on an IncF plasmid as revealed by nanopore sequencing. Antimicrob Agents Chemother 62. https://doi.org/10.1128/AAC.00110-18.
21. Goodman KES, Simner PJ, Tamma PD, Milstone AM. 2016. Infection control implications of heterogeneous resistance mechanisms in carbapenem-resistant Enterobacteriaceae (CRE). Expert Rev Anti Infect Ther 14:95–108. https://doi.org/10.1586/14787210.2016.1106940.
22. Mathers A. 2016. Mobilization of carbapenemase-mediated resistance in Enterobacteriaceae. Microbiol Spectr 4. https://doi.org/10.1128/microbiolspec.EI10-0010-2015.
23. Cuzon G, Naas T, Nordmann P. 2011. Functional characterization of Tn4401, a Tn3-based transposon involved in blaKPC gene mobilization. Antimicrob Agents Chemother 55:5370–5373. https://doi.org/10.1128/AAC.05202-11.
24. Tangden T, Adler M, Cars O, Sandegren L, Lowdin E. 2013. Frequent emergence of porin-deficient subpopulations with reduced carbapenem susceptibility in ESBL-producing Escherichia coli during exposure to ertapenem in an in vitro pharmacokinetic model. J Antimicrob Chemother 68:1319–1326. https://doi.org/10.1093/jac/dkt044.
25. Adler M, Anjum M, Andersson DI, Sandegren L. 2013. Influence of acquired beta-lactamases on the evolution of spontaneous carbapenem resistance in Escherichia coli. J Antimicrob Chemother 68:51–59. https://doi.org/10.1093/jac/dks368.
26. Girlich D, Poirel L, Nordmann P. 2009. CTX-M expression and selection of ertapenem resistance in Klebsiella pneumoniae and Escherichia coli. Antimicrob Agents Chemother 53:832–834. https://doi.org/10.1128/AAC.01007-08.
27. Goessens WH, van der Bij AK, van Boxtel R, Pitout JD, van Ulsen P, Melles DC, Tommassen J. 2013. Antibiotic trapping by plasmid-encoded CMY-2 beta-lactamase combined with reduced outer membrane permeability as a mechanism of carbapenem resistance in Escherichia coli. Antimicrob Agents Chemother 57:3941–3949. https://doi.org/10.1128/AAC.02459-12.
28. van Boxtel R, Wattel AA, Arenas J, Goessens WH, Tommassen J. 2017. Acquisition of carbapenem resistance by plasmid-encoded-AmpC-expressing Escherichia coli. Antimicrob Agents Chemother 61:e01413-16. https://doi.org/10.1128/AAC.01413-16.
29. Partridge SR, Kwong SM, Firth N, Jensen SO. 2018. Mobile genetic elements associated with antimicrobial resistance. Clin Microbiol Rev 31:e00088-17. https://doi.org/10.1128/CMR.00088-17.
30. Ma P, He LL, Pironti A, Laibinis HH, Ernst CM, Manson AL, Bhattacharyya RP, Earl AM, Livny J, Hung DT. 2021. Genetic determinants facilitating the evolution of resistance to carbapenem antibiotics. Elife 10:e67310. https://doi.org/10.7554/eLife.67310.
31. Patiño-Navarrete R, Rosinski-Chupin I, Cabanel N, Gauthier L, Takissian J, Madec J-Y, Hamze M, Bonnin RA, Naas T, Glaser P. 2020. Stepwise evolution and convergent recombination underlie the global dissemination of carbapenemase-producing Escherichia coli. Genome Med 12:10. https://doi.org/10.1186/s13073-019-0699-6.
32. Nicoloff H, Hjort K, Levin BR, Andersson DI. 2019. The high prevalence of antibiotic heteroresistance in pathogenic bacteria is mainly caused by gene amplification. Nat Microbiol 4:504–514. https://doi.org/10.1038/s41564-018-0342-0.
33. Rodriguez-Villodres A, Gil-Marques ML, Alvarez-Marin R, Bonnin RA, Pachon-Ibanez ME, Aguilar-Guisado M, Naas T, Aznar J, Pachon J, Lepe JA, Smani Y. 2019. Extended-spectrum resistance to beta-lactams/beta-lactamase inhibitors (ESRI) evolved from low-level resistant Escherichia coli. J Antimicrob Chemother 75:77–85. https://doi.org/10.1093/jac/dkz393.
34. Karlsson M, Lutgring JD, Ansari U, Lawsin A, Albrecht V, McAllister G, Daniels J, Lonsway D, McKay S, Beldavs Z, Bower C, Dumyati G, Gross A, Jacob J, Janelle S, Kainer MA, Lynfield R, Phipps EC, Schutz K, Wilson L, Witwer ML, Bulens SN, Walters MS, Duffy N, Kallen AJ, Elkins CA, Rasheed JK. 2022. Molecular characterization of carbapenem-resistant *Enterobacterales* collected in the United States. Microb Drug Resist 41:63–70. https://doi.org/10.1089/mdr.2021.0106.].

35. Guérin F, Isnard C, Cattoir V, Giard JC. 2015. Complex regulation pathways of AmpC-mediated β-lactam resistance in Enterobacter cloacae complex. Antimicrob Agents Chemother 59:7753–7761. https://doi.org/10.1128/AAC.01729-15.
36. Clermont O, Christenson JK, Denamur E, Gordon DM. 2013. The Clermont Escherichia coli phylo-typing method revisited: improvement of specificity and detection of new phylo-groups. Environ Microbiol Rep 5:58–65. https://doi.org/10.1111/1758-2229.12019.
37. Hall MN, Silhavy TJ. 1981. The ompB locus and the regulation of the major outer membrane porin proteins of Escherichia coli K12. J Mol Biol 146:23–43. https://doi.org/10.1016/0022-2836(81)90364-8.
38. Livermore DM, Day M, Cleary P, Hopkins KL, Toleman MA, Wareham DW, Wiuff C, Doumith M, Woodford N. 2019. OXA-1 beta-lactamase and non-susceptibility to penicillin/beta-lactamase inhibitor combinations among ESBL-producing Escherichia coli. J Antimicrob Chemother 74:326–333. https://doi.org/10.1093/jac/dky453.
39. Henderson A, Paterson DL, Chatfield MD, Tambyah PA, Lye DC, De PP, Lin RTP, Chew KL, Yin M, Lee TH, Yilmaz M, Cakmak R, Alenazi TH, Arabi YM, Falcone M, Bassetti M, Righi E, Rogers BA, Kanj SS, Bhally H, Iredell J, Mendelson M, Boyles TH, Looke DFM, Runnegar NJ, Miyakis S, Walls G, Khamis MAI, Zikri A, Crowe A, Ingram PR, Daneman N, Griffin P, Athan E, Roberts L, Beatson SA, Peleg AY, Cottrell K, Bauer MJ, Tan E, Chaw K, Nimmo GR, Harris-Brown T, Harris PNA, Newton P, Wren H, Graham M, Korman T, Aljohani SM, Alalwan B, MERINO Trial Investigators and the Australasian Society for Infectious Disease Clinical Research Network (ASID-CRN), et al. 2021. Association between minimum inhibitory concentration, beta-lactamase genes and mortality for patients treated with piperacillin/tazobactam or meropenem from the MERINO study. Clinical Infectious Diseases 73:e3842–e3850. https://doi.org/10.1093/cid/ciaa1479.
40. Harmer CJ, Pong CH, Hall RM. 2020. Structures bounded by directly-oriented members of the IS26 family are pseudo-compound transposons. Plasmid 111:102530. https://doi.org/10.1016/j.plasmid.2020.102530.
41. Harmer CJ, Moran RA, Hall RM. 2014. Movement of IS26-associated antibiotic resistance genes occurs via a translocatable unit that includes a single IS26 and preferentially inserts adjacent to another IS26. mBio 5:e01801-14–e01814. https://doi.org/10.1128/mBio.01801-14.
42. Harmer CJ, Hall RM. 2016. IS26-mediated formation of transposons carrying antibiotic resistance genes. mSphere 1:e00038-16. https://doi.org/10.1128/mSphere.00038-16.
43. David S, Reuter S, Harris SR, Glasner C, Feltwell T, Argimon S, Abudahab K, Goater R, Giani T, Errico G, Aspbury M, Sjunnebo S, Feil EJ, Rossolini GM, Aanensen DM, Grundmann H, Eu SWG, Group ES. 2019. Epidemic of carbapenem-resistant Klebsiella pneumoniae in Europe is driven by nosocomial spread. Nat Microbiol 4:1919–1929. https://doi.org/10.1038/s41564-019-0492-8.
44. Buckner MM, Saw HT, Osagie RN, McNally A, Ricci V, Wand ME, Woodford N, Ivens A, Webber MA, Piddock LJ. 2018. Clinically relevant plasmid-host interactions indicate that transcriptional and not genomic modifications ameliorate fitness costs of Klebsiella pneumoniae carbapenemase-carrying plasmids. mBio 9:e02303-17. https://doi.org/10.1128/mBio.02303-17.
45. Knopp M, Andersson DI. 2015. Amelioration of the fitness costs of antibiotic resistance due to reduced outer membrane permeability by upregulation of alternative porins. Mol Biol Evol 32:3252–3263. https://doi.org/10.1093/molbev/msv195.
46. Adler M, Anjum M, Berg OG, Andersson DI, Sandegren L. 2014. High fitness costs and instability of gene duplications reduce rates of evolution of new genes by duplication-divergence mechanisms. Mol Biol Evol 31:1526–1535. https://doi.org/10.1093/molbev/msu111.
47. Black CA, So W, Dallas SS, Gawrys G, Benavides R, Aguilar S, Chen C-J, Shurko JF, Lee GC. 2021. Predominance of non-carbapenemase producing carbapenem-resistant Enterobacterales in South Texas. Front Microbiol 11:3629. https://doi.org/10.3389/fmicb.2020.623574.
48. Webb BJ, Majers J, Healy R, Jones PB, Butler AM, Snow G, Forsyth S, Lopansri BK, Ford CD, Hoda D. 2020. Antimicrobial stewardship in a hematological malignancy unit: carbapenem reduction and decreased vancomycin-resistant Enterococcus infection. Clinical Infectious Diseases 71:960–967. https://doi.org/10.1093/cid/ciz900.
49. Avershina E, Sharma P, Taxt AM, Singh H, Frye SA, Paul K, Kapil A, Naseer U, Kaur P, Ahmad R. 2021. AMR-Diag: neural network based genotype-to-phenotype prediction of resistance towards beta-lactams in Escherichia coli and Klebsiella pneumoniae. Comput Struct Biotechnol J 19:1896–1906. https://doi.org/10.1016/j.csbj.2021.03.027.
50. Tamma PD, Fan Y, Bergman Y, Pertea G, Kazmi AQ, Lewis S, Carroll KC, Schatz MC, Timp W, Simner PJ. 2019. Applying rapid whole-genome sequencing to predict phenotypic antimicrobial susceptibility testing results among carbapenem-resistant Klebsiella pneumoniae clinical isolates. Antimicrob Agents Chemother 63:e01923-18. https://doi.org/10.1128/AAC.01923-18.
51. Bulman ZP, Krapp F, Pincus NB, Wenzler E, Murphy KR, Qi C, Ozer EA, Hauser AR. 2021. Genomic features associated with the degree of phenotypic resistance to carbapenems in carbapenem-resistant Klebsiella pneumoniae. mSystems 6. https://doi.org/10.1128/mSystems.00194-21.
52. Zienkiewicz M, Kern-Zdanowicz I, Carattoli A, Gniadkowski M, Cegłowski P. 2013. Tandem multiplication of the IS26-flanked amplicon with the bla(SHV-5) gene within plasmid p1658/97. FEMS Microbiol Lett 341:27–36. https://doi.org/10.1111/1574-6968.12084.
53. CLSI. 2018. Performance Standards for Antimicrobial Susceptibility Testing. Clinical and Laboratory Standards Institute, Wayne, PA.
54. Parks DH, Imelfort M, Skennerton CT, Hugenholtz P, Tyson GW. 2015. CheckM: assessing the quality of microbial genomes recovered from isolates, single cells, and metagenomes. Genome Res 25:1043–1055. https://doi.org/10.1101/gr.186072.114.
55. Pedersen BS, Quinlan AR. 2018. Mosdepth: quick coverage calculation for genomes and exomes. Bioinformatics 34:867–868. https://doi.org/10.1093/bioinformatics/btx699.
56. Tonkin-Hill G, Macalasdair N, Ruis C, Weimann A, Horesh G, Lees JA, Gladstone RA, Lo S, Beaudoin C, Floto RA, Frost SDW, Corander J, Bentley SD, Parkhill J. 2020. Producing polished prokaryotic pangenomes with the Panaroo pipeline. Genome Biol 21. https://doi.org/10.1186/s13059-020-02090-4.
57. Minh BQ, Schmidt HA, Chernomor O, Schrempf D, Woodhams MD, von Haeseler A, Lanfear R. 2020. IQ-TREE 2: new models and efficient methods for phylogenetic inference in the genomic era. Mol Biol Evol 37:1530–1534. https://doi.org/10.1093/molbev/msaa015.
58. Kalyaanamoorthy S, Minh BQ, Wong TKF, Von Haeseler A, Jermiin LS. 2017. ModelFinder: fast model selection for accurate phylogenetic estimates. Nat Methods 14:587–589. https://doi.org/10.1038/nmeth.4285.
59. Hoang DT, Chernomor O, Von Haeseler A, Minh BQ, Vinh LS. 2018. UFBoot2: improving the ultrafast bootstrap approximation. Mol Biol Evol 35:518–522. https://doi.org/10.1093/molbev/msx281.
60. Tonkin-Hill G, Lees JA, Bentley SD, Frost SDW, Corander J. 2018. RhierBAPS: an R implementation of the population clustering algorithm hierBAPS. Wellcome Open Res 3:93. https://doi.org/10.12688/wellcomeopenres.14694.1.
61. Lam MMC, Wick RR, Watts SC, Cerdeira LT, Wyres KL, Holt KE. 2021. A genomic surveillance framework and genotyping tool for Klebsiella pneumoniae and its related species complex. Nat Commun 12:4188. https://doi.org/10.1038/s41467-021-24448-3.
62. Ondov BD, Treangen TJ, Melsted P, Mallonee AB, Bergman NH, Koren S, Phillippy AM. 2016. Mash: fast genome and metagenome distance estimation using MinHash. Genome Biol 17:132. https://doi.org/10.1186/s13059-016-0997-x.
63. Joensen KG, Tetzschner AM, Iguchi A, Aarestrup FM, Scheutz F. 2015. Rapid and easy in silico serotyping of Escherichia coli isolates by use of whole-genome sequencing data. J Clin Microbiol 53:2410–2426. https://doi.org/10.1128/JCM.00008-15.
64. Larsen MV, Cosentino S, Rasmussen S, Friis C, Hasman H, Marvig RL, Jelsbak L, Sicheritz-Pontén T, Ussery DW, Aarestrup FM, Lund O. 2012. Multilocus sequence typing of total-genome-sequenced bacteria. J Clin Microbiol 50:1355–1361. https://doi.org/10.1128/JCM.06094-11.
65. Beghain J, Bridier-Nahmias A, Le Nagard H, Denamur E, Clermont O. 2018. ClermonTyping: an easy-to-use and accurate in silico method for Escherichia genus strain phylotyping. Microb Genom 4. https://doi.org/10.1099/mgen.0.000192.
66. Siguier P, Perochon J, Lestrade L, Mahillon J, Chandler M. 2006. ISfinder: the reference centre for bacterial insertion sequences. Nucleic Acids Res 34:D32–D36. https://doi.org/10.1093/nar/gkj014.
67. Clausen PTLC, Zankari E, Aarestrup FM, Lund O. 2016. Benchmarking of methods for identification of antimicrobial resistance genes in bacterial whole genome data. J Antimicrob Chemother 71:2484–2488. https://doi.org/10.1093/jac/dkw184.
68. Clausen PTLC, Aarestrup FM, Lund O. 2018. Rapid and precise alignment of raw reads against redundant databases with KMA. BMC Bioinformatics 19:307. https://doi.org/10.1186/s12859-018-2336-6.
69. Robertson J, Nash JHE. 2018. MOB-suite: software tools for clustering, reconstruction and typing of plasmids from draft assemblies. Microb Genom 4:e000206. https://doi.org/10.1099/mgen.0.000206.
70. Jain C, Rodriguez-R LM, Phillippy AM, Konstantinidis KT, Aluru S. 2018. High throughput ANI analysis of 90K prokaryotic genomes reveals clear species boundaries. Nat Commun 9:5114. https://doi.org/10.1038/s41467-018-07641-9.

71. Gascuel O. 1997. BIONJ: an improved version of the NJ algorithm based on a simple model of sequence data. Mol Biol Evol 14:685–695. https://doi.org/10.1093/oxfordjournals.molbev.a025808.
72. Paradis E, Schliep K. 2019. ape 5.0: an environment for modern phylogenetics and evolutionary analyses in R. Bioinformatics 35:526–528. https://doi.org/10.1093/bioinformatics/bty633.
73. Guy L, Roat Kultima J, Andersson SGE. 2010. genoPlotR: comparative gene and genome visualization in R. Bioinformatics 26:2334–2335. https://doi.org/10.1093/bioinformatics/btq413.
74. Hanson BM, Johnson JS, Leopold SR, Sodergren E, Weinstock GM. 2019. SVants – A long-read based method for structural variation detection in bacterial genomes. bioRxiv 1:822312.